

Review

Not peer-reviewed version

---

# Integrated Photonic Sensors for The Detection of Toxic Gases - A Review

---

[Muhammad A. Butt](#)<sup>\*</sup> and [Ryszard Piramidowicz](#)

Posted Date: 12 June 2024

doi: 10.20944/preprints202406.0864.v1

Keywords: Gas sensor; integrated photonic sensor; evanescent field absorption; functional material



Preprints.org is a free multidiscipline platform providing preprint service that is dedicated to making early versions of research outputs permanently available and citable. Preprints posted at Preprints.org appear in Web of Science, Crossref, Google Scholar, Scilit, Europe PMC.

Copyright: This is an open access article distributed under the Creative Commons Attribution License which permits unrestricted use, distribution, and reproduction in any medium, provided the original work is properly cited.

Review

# Integrated Photonic Sensors for The Detection of Toxic Gases- A Review

Muhammad A. Butt \* and R. Piramidowicz

Institute of Microelectronics and Optoelectronics, Warsaw University of Technology, Koszykowa 75, 00-662, Warsaw, poland

\* Correspondence: ali.butt@pw.edu.pl

**Abstract:** Gas sensing is crucial for detecting hazardous gases in industrial environments, ensuring safety and preventing accidents. Additionally, it plays a vital role in environmental monitoring and control, helping to mitigate pollution and protect public health. Integrated photonic gas sensors are important due to their high sensitivity, rapid response time, and compact size, enabling precise recognition of gas concentrations in real-time. These sensors leverage photonic technologies, such as waveguides and resonators, to enhance performance over traditional gas sensors. Advancements in materials and fabrication techniques could further improve their efficiency, making them invaluable for environmental monitoring, industrial safety, and healthcare diagnostics. In this review, we delved into photonic gas sensors that operate based on the principles of evanescent field absorption (EFA) and wavelength interrogation methods. These advanced sensing mechanisms allow for highly sensitive and selective gas detection, leveraging the interplay of light with gas molecules to produce precise measurements.

**Keywords:** Gas sensor; integrated photonic sensor; evanescent field absorption; functional material

## 1. Introduction

Indoor and outdoor gas sensing is crucial for public health, safety, and environmental protection [1,2]. Indoors, gas sensors detect pollutants such as carbon monoxide (CO), volatile organic compounds (VOCs), and radon, which can reach hazardous levels and cause serious health issues like respiratory problems, neurological damage, or even fatalities [3]. Continuous indoor gas sensing ensures good air quality in homes, offices, and industrial buildings, verifying the effectiveness of ventilation systems and protecting occupants from toxic exposures. Outdoors, gas sensors monitor air quality and track emissions of harmful gases like sulfur dioxide, nitrogen oxides, and ozone, which contribute to smog, acid rain, and climate change, negatively impacting ecosystems and human health [4]. These sensors help regulatory agencies enforce air quality standards, inform policy decisions, and increase public awareness of pollution levels. In industrial settings, both indoor and outdoor gas sensing is vital for detecting hazardous gas leaks, ensuring safe working conditions, and preventing environmental contamination [5]. Comprehensive gas sensing is therefore essential for protecting health, promoting environmental stewardship, and ensuring regulatory compliance across various sectors [6–9].

Integrated photonic sensors have revolutionized the field of gas sensing by leveraging the principles of photonics to provide highly sensitive, fast, and reliable recognition of various gases [10–12]. These sensors utilize the interplay between light and gas molecules to identify and quantify gases with exceptional precision. The amalgamation of photonic components onto a single chip has significantly miniaturized gas sensors, making them more compact, energy-efficient, and cost-effective compared to traditional methods. This miniaturization is predominantly significant in products requiring portable or wearable devices, where size, weight, and power consumption are critical factors. The primary significance of gas sensing with integrated photonic sensors lies in their high sensitivity and specificity. Photonic sensors can detect minute concentrations of gases, often in the parts-per-million (ppm) or parts-per-billion (ppb) range, which is essential for applications in

environmental surveillance, industrial safety, and medical diagnostics [13]. For instance, detecting trace levels of dangerous gases in industrial environments can avert accidents and ensure worker safety. In environmental monitoring, these sensors can track pollutants with high accuracy, contributing to better air quality management and public health [14–16]. In medical diagnostics, integrated photonic sensors can be used for non-invasive breath analysis to detect biomarkers for various diseases, enabling early diagnosis and personalized treatment.

Another significant advantage of integrated photonic sensors is their rapid response time and real-time monitoring capabilities. The interplay of light with gas molecules occurs at the speed of light, allowing for instantaneous detection and continuous monitoring of gas concentrations. This rapid response is crucial in scenarios where immediate detection is required, such as in detecting gas leaks or monitoring volatile organic compounds (VOCs) in industrial processes [17]. Additionally, the ability to provide real-time data enhances the effectiveness of monitoring systems, allowing for timely interventions and informed decision-making. Furthermore, the versatility and scalability of integrated photonic sensors make them suitable for a broad spectrum of uses. These sensors can be designed to target specific gases by tuning the photonic components, such as lasers and waveguides (WGs), to the characteristic absorption wavelengths of the desired gases [18]. This tunability, combined with the ability to integrate several sensing elements on a single chip, permits the simultaneous detection of multiple gases, providing comprehensive monitoring solutions. The scalability of photonic integration also supports mass production, reducing costs and enabling widespread adoption in various industries.

The paper is organized as follows: Section 2 provides a brief description of indoor and outdoor toxic gases and their impact on human health. Section 3 discusses the widely used optical WG architectures for gas sensing applications. The focus of the paper is on two gas sensing mechanisms, namely evanescent field absorption and the wavelength interrogation method, which are detailed in Section 4. Section 5 covers other types of photonic gas sensors, such as those based on metasurfaces, optical fibers, and photoacoustic spectroscopy. The fabrication methods for integrated photonic sensors are outlined in Section 6. Section 7 addresses the challenges and prospects of integrated photonic gas sensors. Finally, the paper concludes with a summary in Section 8.

## 2. Indoor and Outdoor Toxic Gases

Indoor and outdoor environments both harbor a variety of toxic gases that pose significant health risks to humans. Indoors, common toxic gases include CO, which is produced by faulty furnaces, gas stoves, fireplaces, and tobacco smoke (Figure 1). Even at low levels, CO can cause headaches and dizziness, while high levels can be fatal [19]. Radon, a radioactive gas from the natural decay of uranium in the soil, infiltrates homes through cracks in floors and walls, and is the leading cause of lung cancer among non-smokers [20]. VOCs, emitted from household products like paints, cleaning supplies, and furniture, can lead to respiratory issues, headaches, dizziness, and long-term health effects including cancer [21]. Nitrogen dioxide (NO<sub>2</sub>), produced by combustion appliances like gas stoves and heaters, exacerbates asthma and reduces lung function [22]. Formaldehyde, found in building materials, tobacco smoke, and various household products, causes eye, nose, and throat irritation and is a known carcinogen. Ammonia (NH<sub>3</sub>), released from cleaning products, textiles, and plastics, causes respiratory irritation, coughing, and throat irritation [23].

On the other hand, outdoor environments are similarly affected by toxic gases. CO from vehicle exhaust and industrial processes can cause cardiovascular and neurological damage. NO<sub>2</sub>, produced by vehicles, power plants, and industrial emissions, irritates the respiratory system and reduces lung function. Sulfur dioxide (SO<sub>2</sub>), released from burning fossil fuels and industrial activities, causes respiratory problems and aggravates heart disease. Ozone (O<sub>3</sub>), a secondary pollutant formed by chemical reactions between VOCs and nitrogen oxides (NO<sub>x</sub>) in the presence of sunlight, leads to respiratory issues and exacerbates asthma [24]. VOCs, emitted from industrial processes, vehicle exhaust, and chemical solvents, cause headaches, dizziness, respiratory tract irritation, and some are carcinogenic [25]. Particulate matter (PM), though not a gas, carries adsorbed toxic gases and fine particles (PM<sub>2.5</sub>) that penetrate deep into the lungs, causing cardiovascular and respiratory diseases

and increasing mortality. Hydrogen sulfide ( $H_2S$ ), produced by industrial activities and the decomposition of organic matter, causes respiratory irritation, headaches, and neurological damage [26].  $NH_3$ , released from agricultural activities and industrial processes, irritates the respiratory system and eyes [27]. Benzene, a component of vehicle exhaust and industrial emissions, is a known carcinogen that causes leukemia and other blood disorders. Lead, emitted from industrial processes and historically from gasoline additives, causes neurological and developmental issues, particularly in children. Effective ventilation, emission controls, and regular supervising are crucial in mitigating the health risks associated with these harmful gases, both indoors and outdoors.

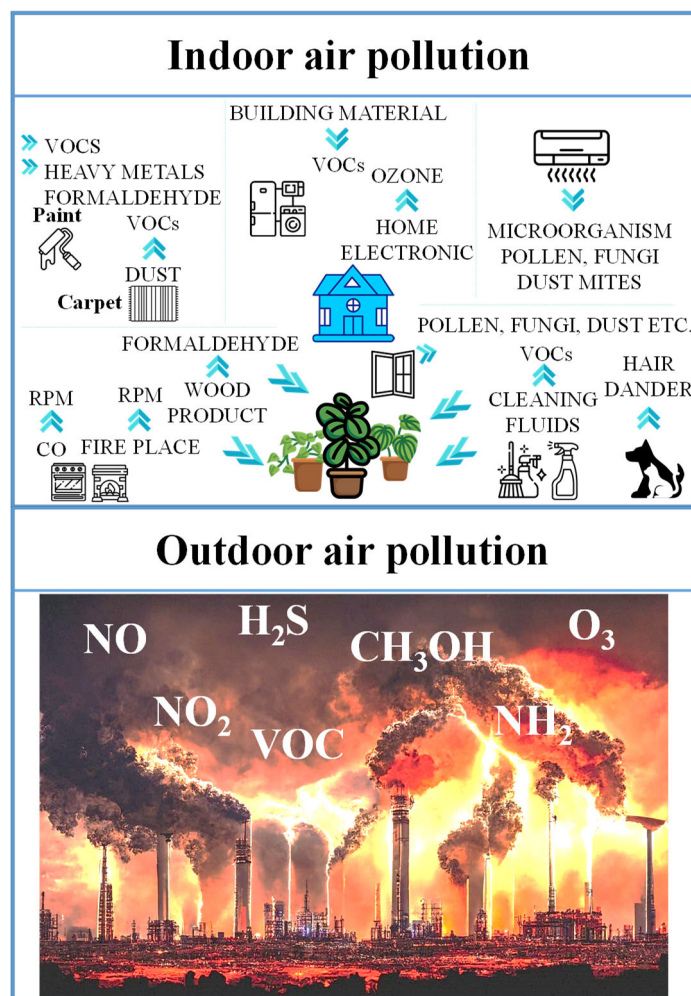


Figure 1. Graphical illustration depicting indoor (Top) and outdoor (Bottom) air pollution.

### 3. Types of Optical WG Architectures Widely Used for Gas Sensing

WG architectures for gas sensors are ingeniously designed to maximize light-matter interplay, thereby enhancing sensitivity and enabling precise gas detection. One prominent architecture is the planar WG, where light is confined in a thin film on a substrate [28]. The evanescent field extends slightly beyond the WG, interacting with the surrounding gas [29]. This design can be further enhanced using materials with high refractive index contrasts, such as silicon (Si) or silicon nitride (SiN), which increase the strength of the evanescent field and thus improve sensitivity. Additionally, the surface of planar WGs can be functionalized with selective coatings to bind specific gas molecules, enhancing the sensor's selectivity and response [30]. The incidence of light on the edge of a glass coverslip for a microscope slide, deposited with a thin film on both faces, permitted the excitation of two resonances in each polarization state of the input light, TE and TM. This dually nanocoated WG was used for the simultaneous detection of two different parameters through further deposition of suitable materials on each face (Figure 2 (a)) [31]. For instance, the detection of temperature and

humidity was demonstrated using polydimethylsiloxane (PDMS) and agarose coatings, respectively, paving the way for the expansion of other dual-parameter sensors and even more parameters when each face of the coverslip is patterned. Additionally, the device was optimized to position two resonances in the near-infrared (NIR) and two resonances in the visible region, with sensitivities of 0.34 nm/°C and 0.23 nm/%RH in the visible region and 1.16 nm/°C and 0.34 nm/%RH in the NIR, respectively, showcasing the potential of the device for use in both spectral ranges and permitting the progress of sensors based on multiple resonances, each linked with a different parameter to be sensed [31].

Slot WGs and subwavelength grating (SWG) WGs are innovative structures that hold promise for gas sensing applications due to their exceptional properties. Slot WGs consist of a narrow slot between two high-index materials, typically Si or SiN, allowing for strong confinement of light in the slot region (Figure 2 (b)) [32–34], [35]. The E-field confinement in the slot WG is displayed in Figure 2 (c) [36]. This confinement enhances the interplay between light and gas molecules, leading to increased sensitivity. Moreover, the slot region can be functionalized with materials that selectively bind target gas molecules, further enhancing the sensor's specificity.

SWG WGs, on the other hand, utilize periodic structures with feature sizes smaller than the wavelength of light, enabling precise control over the dispersion and confinement of light [37]. By engineering the grating parameters, such as period and duty cycle, the WG properties can be tailored to achieve desired sensing characteristics [38–40]. Both slot WGs and SWG WGs offer opportunities for highly sensitive and selective gas sensing platforms, holding potential for advancements in environmental surveillance, industrial process control, and healthcare diagnostics. A photonic array of resonant circular dielectric WGs with SWG was proposed as a robust and sensitive topological chemical sensor [41]. The device was tailored to identify trace amounts of a given chemical species through photonic edge modes, which are impervious to most sources of disorder. A simulation in the MIR was performed, accounting for the absorption loss introduced by chemical molecules in contact with a strongly coupled photonic lattice of resonators. Due to the topological nature of the device, its chemical sensitivity scaled linearly with the system size, reaching ppb range at the millimeter scale. These findings suggested that topological chemical sensors could allow the expansion of novel on-chip integrated photonic sensing technologies. A SWG WG was employed to enhance light-chemical interplay (Figure 2 (d)). The strong coupling bridge resonator unit mediated the coupling between lattice sites in the array (Figure 2 (e)). The design featured a dielectric circular array with designated source and drain for transmitting power. Gray rings represented lattice sites, while black rings indicated bridge resonators connecting these sites. All rings functioned as SWG WGs, as illustrated in the inset (Figure 2 (f)). Red lines marked the topologically protected modes propagating along the edges of the array. The inset depicted a unit cell of the lattice [41].

Photonic crystal (PhC) WGs represent a highly sensitive architecture due to their ability to confine light in very small volumes [42,43]. These WGs consist of periodic dielectric structures that create photonic bandgaps, trapping and guiding light in defect regions (Figure 2 (g)) [44]. The strong localization of light in these structures enhances the interplay with the gas molecules, leading to significant changes in the optical properties even with minute quantities of gas. Moreover, the PhC can be intended to operate at specific wavelengths where the target gas has strong absorption, further boosting the sensor's sensitivity [45–47].

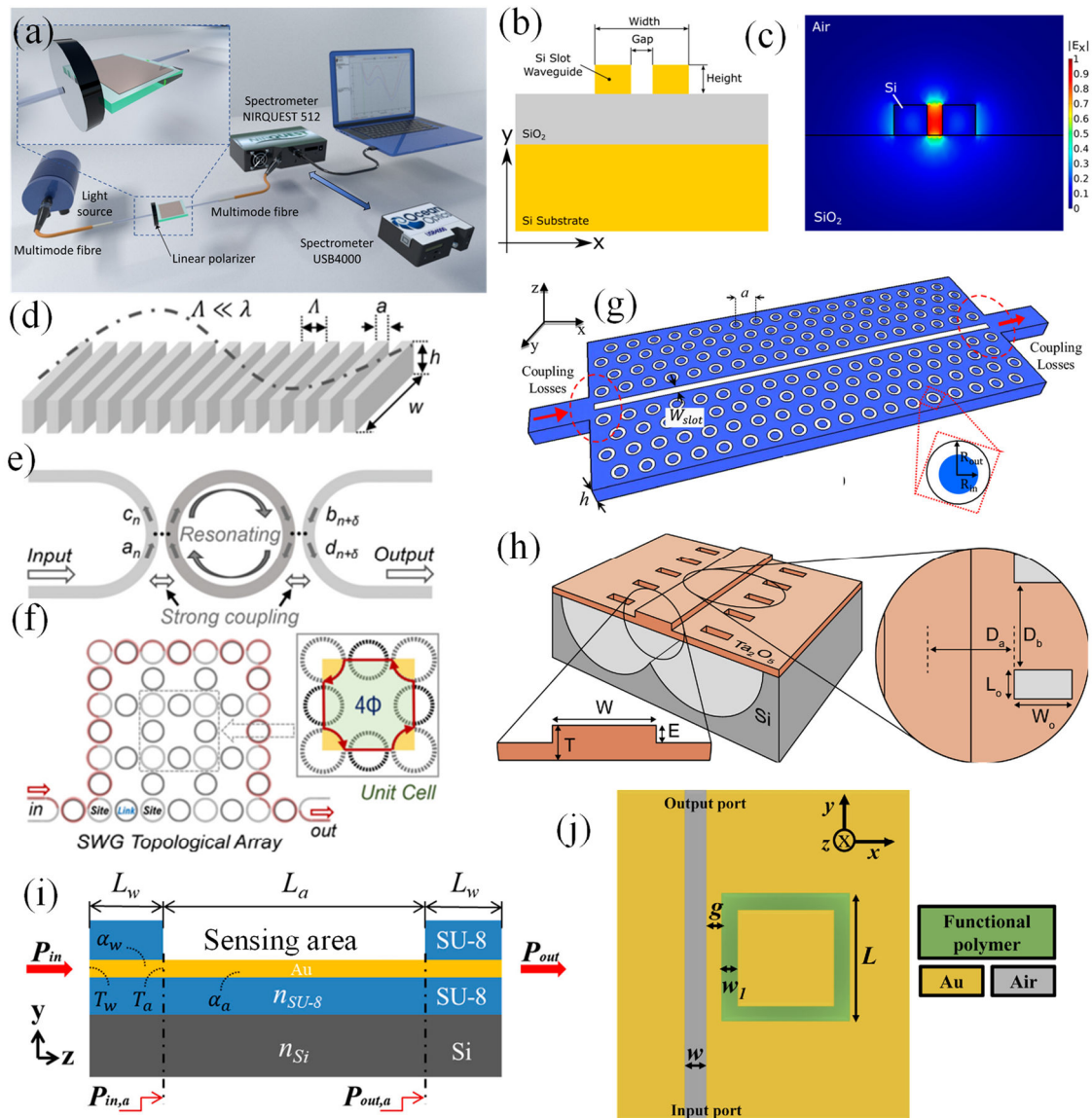


**Figure 2.** Different WG configurations for sensing purposes, (a) Planar WG, (b) Slot WG and E-field distribution (c) [36], (d) SWG WG [41], (e) Ring resonator for coupling [41], (f) SWG WG based ring resonator structures for sensing [41], (g) Photonic crystal WG [44], (h) Suspended membrane WG [49], (i) Surface plasmon WG [52], (j) MIM WG [53].

A suspended membrane WG for gas sensing is another advanced technology designed to enhance the detection and measurement of gas concentrations with high sensitivity and selectivity [48]. This WG consists of a thin, flexible membrane suspended over a substrate, allowing it to interact more directly with the surrounding gas molecules (Figure 2 (h)) [49]. The membrane's material is typically chosen for its specific interaction properties with the target gas, and its suspended nature reduces background interference from the substrate, improving detection accuracy [50]. When gas molecules adsorb onto the membrane, they induce changes in its optical or mechanical properties, such as refractive index or vibration frequency, which can be measured and correlated to gas concentration [49]. This configuration not only improves the sensor's sensitivity and response time but also enables miniaturization, making it suitable for portable and remote sensing purposes [51].

Surface plasmon (SP) WGs combine the advantages of plasmonics and WG technology to attain high sensitivity [54]. In these sensors, a metal layer, in general gold or silver, is integrated with a dielectric WG (Figure 2 (i)) [52]. The interplay of light with the metal surface excites surface plasmons, which are highly sensitive to changes in the refractive index near the surface. When gas molecules adsorb onto the metal surface, they alter the local refractive index, shifting the surface plasmon

resonance (SPR) condition. This shift can be detected with high precision, making SP WGs particularly effective for detecting low concentrations of gases. Additionally, metal-insulator-metal (MIM) configuration [55] is also employed as highly sensitive WG structures (Figure 1 (j)) [53].

#### 4. Two Widely Employed Gas Sensing Mechanisms

Gas sensing mechanisms such as evanescent field absorption (EFA) and wavelength interrogation offer distinct yet complementary approaches to detecting gases using optical WGs. When gas molecules are present near the WG surface, they interact with the evanescent field, leading to absorption at specific wavelengths characteristic of the gas. This absorption causes measurable changes in the light's intensity, which can be correlated to gas concentration. On the other hand, the wavelength interrogation method involves observing shifts in the wavelength of light that resonate within the WG, often using structures like Mach-Zehnder interferometer (MZI) [13] or ring resonators [56]. In this case, functional polymers like polyhexamethylene biguanide (PHMB) play a crucial role in enhancing the sensitivity and selectivity of gas sensors. When used in gas sensors, PHMB can be coated onto the surface of a sensing substrate, such as an optical WG [57,58]. Upon exposure to the target gas, PHMB undergoes changes in its physical or chemical properties, such as, refractive index alteration, or conductivity variation. These changes can then be detected by the sensor's transduction mechanism—be it optical, electrical, or another modality—allowing for the precise quantification of the gas concentration [59]. The high affinity of PHMB for specific gases, combined with its robustness and stability, makes it particularly effective for applications in environmental surveillance, industrial safety, and medical diagnostics, where accurate and reliable gas detection is paramount. Both mechanisms offer high sensitivity and specificity, making them valuable for applications ranging from environmental surveillance to industrial safety and medical diagnostics.

##### 4.1. Gas Sensors based on The Mechanism of EFA

The mid-infrared (MIR) region, typically defined as the wavelength range from 2.5 to 25 micrometers, is particularly significant for gas sensing applications due to its strong absorption characteristics for many molecular gases [60,61]. The absorption wavelengths listed in Table 1 are representative of strong absorption peaks within the MIR region [60].

**Table 1.** Absorption wavelengths for various gases in the MIR region.

Gas	Absorption Wavelengths ( $\mu\text{m}$ )	Absorption Wavenumbers ( $\text{cm}^{-1}$ )
Carbon Dioxide ( $\text{CO}_2$ )	4.26, 14.99, 15.45	2349, 667, 648
Methane ( $\text{CH}_4$ )	3.31, 7.66	3020, 1305
Water Vapor ( $\text{H}_2\text{O}$ )	2.66, 6.27	3756, 1596
Nitrous Oxide ( $\text{N}_2\text{O}$ )	4.50, 7.80	2222, 1282
Ozone ( $\text{O}_3$ )	9.60, 14.24	1042, 702
Sulfur Dioxide ( $\text{SO}_2$ )	7.34, 8.72	1363, 1147
Ammonia ( $\text{NH}_3$ )	2.97, 9.22	3368, 1085
Carbon Monoxide ( $\text{CO}$ )	4.67	2143
Nitric Oxide ( $\text{NO}$ )	5.30, 5.44	1887, 1838
Formaldehyde ( $\text{HCHO}$ )	5.72, 9.60	1750, 1042

The actual absorption spectrum for each gas is broad and can contain many more peaks. In this spectral region, fundamental vibrational transitions of molecules occur, providing distinct and strong absorption features that can be used to identify and quantify various gases with high sensitivity and specificity. Utilizing the MIR region for gas sensing enables the detection of a wide range of gases, including  $\text{CO}_2$ ,  $\text{CH}_4$ , and VOCs, which have critical absorption bands in this range. Advances in MIR sources, such as quantum cascade lasers, and detectors, like mercury cadmium telluride (MCT) photodiodes, have greatly enhanced the capabilities of MIR gas sensors. These technologies allow for

real-time, in situ monitoring of gas concentrations, making them invaluable in environmental surveillance, industrial process control, and medical diagnostics, where precise and accurate gas detection is crucial.

Integrated photonic sensors utilizing the EFA mechanism represent a sophisticated approach to gas detection, leveraging the interplay between light and gas molecules at the interface of a WG [61]. In these sensors, light is guided through a photonic WG, and a small portion of the light, known as the evanescent field, extends beyond the surface of the WG into the surrounding medium [62]. When gas molecules are present near the WG surface, they interact with this evanescent field, leading to absorption of specific wavelengths of light that correspond to the characteristic absorption spectra of the gas molecules [18,63,64].

Determining the evanescent field ratio (EFR) of a WG is vital for enhancing the performance and accuracy of gas sensors working on the principle of EFA [65]. The EFR quantifies the extent to which the optical field penetrates the neighboring gas medium outside the WG core. This penetration enables the sensor to detect variations in the gas's refractive index or absorbance, which are indicative of the presence and concentration of specific gas molecules. A higher EFR leads to a more significant interplay between the light and the gas, thereby improving the sensor's sensitivity and detection limit. Accurately determining this ratio allows for the optimization of the WG design and material properties to maximize the sensor's responsiveness and precision [66].

One of the primary advantages of using the EFA mechanism in integrated photonic sensors is the ability to perform real-time and continuous surveillance of gas concentrations [18,67]. The absorption of light by the gas molecules leads to a measurable change in the intensity or phase of the light propagating through the WG. This change can be detected and analyzed in real time, providing immediate feedback on the presence and concentration of the target gas. This capability is particularly valuable in applications such as industrial safety, where rapid detection of hazardous gases can prevent accidents and ensure timely responses. Furthermore, integrated photonic sensors based on EFA can be miniaturized and integrated into compact, low-power devices. The use of photonic integration allows multiple sensing elements to be combined on a single chip, enabling multi-gas detection and reducing the overall footprint of the sensor system [68]. This miniaturization is advantageous for portable and wearable applications, where space and power are limited. Additionally, the robustness and stability of photonic WGs contribute to the durability and long-term reliability of these sensors, making them suitable for deployment in harsh environments.

Photonic gas sensors operating in the MIR region rely on specific material platforms to achieve efficient detection. Among the prominent materials are chalcogenide glasses, which offer wide transparency windows and high refractive indices, enabling the construction of compact and sensitive sensors. Another significant platform is silicon-on-insulator (SOI) [12], known for its compatibility with complementary metal-oxide-semiconductor (CMOS) technology, facilitating the integration of photonic components with electronic circuits for enhanced functionality and performance. Additionally, III-V semiconductor materials like indium phosphide (InP) [69,70] and gallium arsenide (GaAs) [71] are utilized due to their superior optical properties and compatibility with laser sources, enabling direct on-chip integration of light sources and detectors. These material platforms play a fundamental role in the extension of robust and efficient photonic gas sensors for various applications ranging from environmental monitoring to industrial safety.

The evaluations of CH<sub>4</sub> gas sensors utilizing SOI technology, as illustrated in [18,72], have been thoroughly investigated. However, these studies have revealed a drawback beyond the wavelength of 3.6 μm, where the SiO<sub>2</sub> material experiences high absorption. Subsequently, the implementation of SOI-based WGs in the MIR region has become impractical. Given this limitation, alternative materials with a broad transparency range in the MIR region, as mentioned in [73–75], have emerged as feasible options. Materials such as Ge and CaF<sub>2</sub>, characterized by high-index contrast, have been identified as promising substitutes for CH<sub>4</sub> gas-sensing applications compared to SOI materials. For a thorough understanding of gas-sensor evaluations for various gases, significant contributions have been made in [76,77]. These investigations collectively enrich the broader field of gas-sensing

technologies, offering significant comprehensions into the diverse applications and material considerations necessary for enhancing sensor performance.

Jin et al. developed a chip-scale MIR sensor for detecting hydrocarbon gases [78]. Fabricated using CMOS processes, the sensor utilized amorphous Si (a-Si) optical ridge WGs as illustrated in Figure 3 (a). To assess the optical performance of these WGs, a MIR test station was set up, as publicized in Figure 3 (b). The illumination source utilized was a pulsed laser operating at a 150 kHz repetition rate, with a pulse duration of 10 ns and an average power of 150 mW. A reflective lens collimated the probe light into a fluoride fiber featuring a 9  $\mu\text{m}$  core and 125  $\mu\text{m}$  cladding, which was subsequently butt-coupled into the WG. Precise alignment between the optical fiber and the a-Si WG was ensured using a microscope equipped with a long working distance 10 $\times$  objective lens. The gas delivery system comprised three mass flow controllers (MFCs) to manage the flow rates of  $\text{C}_2\text{H}_2$ ,  $\text{CH}_4$ , and  $\text{N}_2$ , adjusting the analyte concentration by modifying the gas flow ratios. The gas sample was introduced into a sealed PDMS chamber placed on top of the WG sensor, thereby exposing the a-Si WGs to the gas analytes. MIR signals emitted from the WGs were concentrated using a calcium fluoride biconvex lens with a 25 mm focal length and captured by a liquid nitrogen-cooled InSb camera. The WG exhibited a sharp fundamental mode throughout the  $\lambda = 2.70$  to 3.50  $\mu\text{m}$  range. Sensing performance was evaluated by measuring  $\text{CH}_4$  and acetylene, identifying characteristic C–H absorption bands for  $\text{CH}_4$  at  $\lambda = 3.29$ –3.33  $\mu\text{m}$  and for acetylene at  $\lambda = 3.00$ –3.06  $\mu\text{m}$  through spectral mode attenuation. Additionally, real-time surveillance of  $\text{CH}_4$  and acetylene concentrations was demonstrated at  $\lambda = 3.02$  and 3.32  $\mu\text{m}$ . This MIR WG sensor thus enabled precise and instant analysis of hydrocarbon gas mixtures [78].

Two theoretical proposals for optical WG sensors based on slot WG and subwavelength slot (SWGS) utilizing SOS (silicon-on-sapphire) were introduced by Song et al. for  $\text{CO}_2$  detection as presented in Figure 3 (c, d) [61]. The operational wavelength stands at 4.23  $\mu\text{m}$ , corresponding to the maximal absorption line of  $\text{CO}_2$ . Power confinement factor ( $\beta$ ) values exceed 40% and 50%, while propagation loss measures at 0.98 dB/cm and 2.99 dB/cm for the slot WG and SWGS WG, respectively. An inverted tapered structure facilitates the transition from strip WG to slot WG, constituting the sensing absorption region, with coupling efficiency exceeding 90%. Optimal absorption lengths for the slot WG and SWGS WG are 1.02 cm and 0.33 cm, respectively, yielding maximum sensitivities of  $6.66 \times 10^{-5}$  ( $\text{ppm}^{-1}$ ) and  $2.60 \times 10^{-5}$  ( $\text{ppm}^{-1}$ ).

Kazanskiy et al. proposed a polarization-independent design for a hybrid plasmonic waveguide (HPWG) optimized at a 3.392  $\mu\text{m}$  wavelength, corresponding to the absorption line of  $\text{CH}_4$ , as shown in Figure 4(a) [79]. This WG design demonstrated high mode sensitivity ( $S_{\text{mode}}$ ) and EFR for both TE and TM hybrid modes. The modal analysis of the WG was conducted using two-dimensional (2D) and three-dimensional (3D) finite element methods (FEMs). At optimized WG parameters, the TE hybrid mode achieved  $S_{\text{mode}}$  and EFR values of 0.94 and 0.704, respectively, while the TM hybrid mode achieved  $S_{\text{mode}}$  and EFR values of 0.86 and 0.67, respectively. Additionally, both TE and TM hybrid modes exhibited a power dissipation of approximately 3 dB for a 20- $\mu\text{m}$ -long hybrid plasmonic WG at a 60% gas concentration. The inset of Figure 4(a) illustrates the field confinement for both TE and TM polarizations. The proposed WG scheme presented in this study is believed to overcome the limitations associated with polarization-controlled light, making it suitable for use in gas sensing applications.

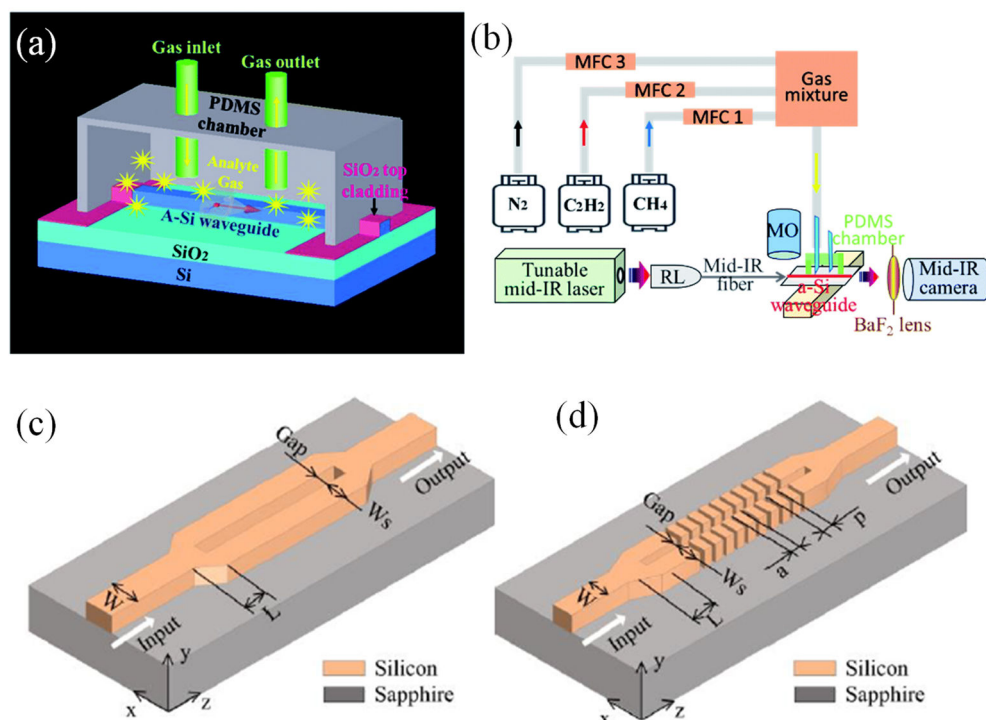


**Figure 3.** (a) Graphical illustration of a-Si ridge WG for hydrocarbon gas detection [78], (b) Gas sensing setup [78], (c) Slot WG structure [61], (d) Subwavelength grating slot WG structure [61].

Nanophotonic WGs have become central to a wide range of optical sensors. These structures channel light along specific paths on photonic chips, enabling light-matter interaction via an evanescent field. Despite their potential, WGs have yet to surpass free-space optics in sensitivity-critical applications like trace gas detection. The primary challenges hindering on-chip gas sensing include short optical path lengths, low interaction strengths, and spurious etalon fringes in spectral transmission. However, Vlk et al. proposed a MIR integrated WG sensor that addresses these issues effectively [67]. This sensor achieved a 107% evanescent field confinement factor in air, surpassing free-space beams in per-length optical interaction. Additionally, minimal facet reflections resulted in a flat spectral background and record-low absorbance noise, rivaling free-space spectroscopy. The sensor's performance was confirmed at  $2.566 \mu\text{m}$ , demonstrating a 7-ppm detection limit for acetylene with just a 2 cm long WG. The WGs were evaluated in an end-fire coupling configuration employing the combined imaging and spectroscopy setup displayed in Figure 4 (b). For the TM polarization, a WG propagation loss of  $6.8 \text{ dB cm}^{-1}$  was measured (Figure 4 (c, d)). This loss was primarily due to light absorption in the  $\text{Ta}_2\text{O}_5$  film caused by residual OH and water, and it is expected to decrease significantly with an optimized film deposition process [67].

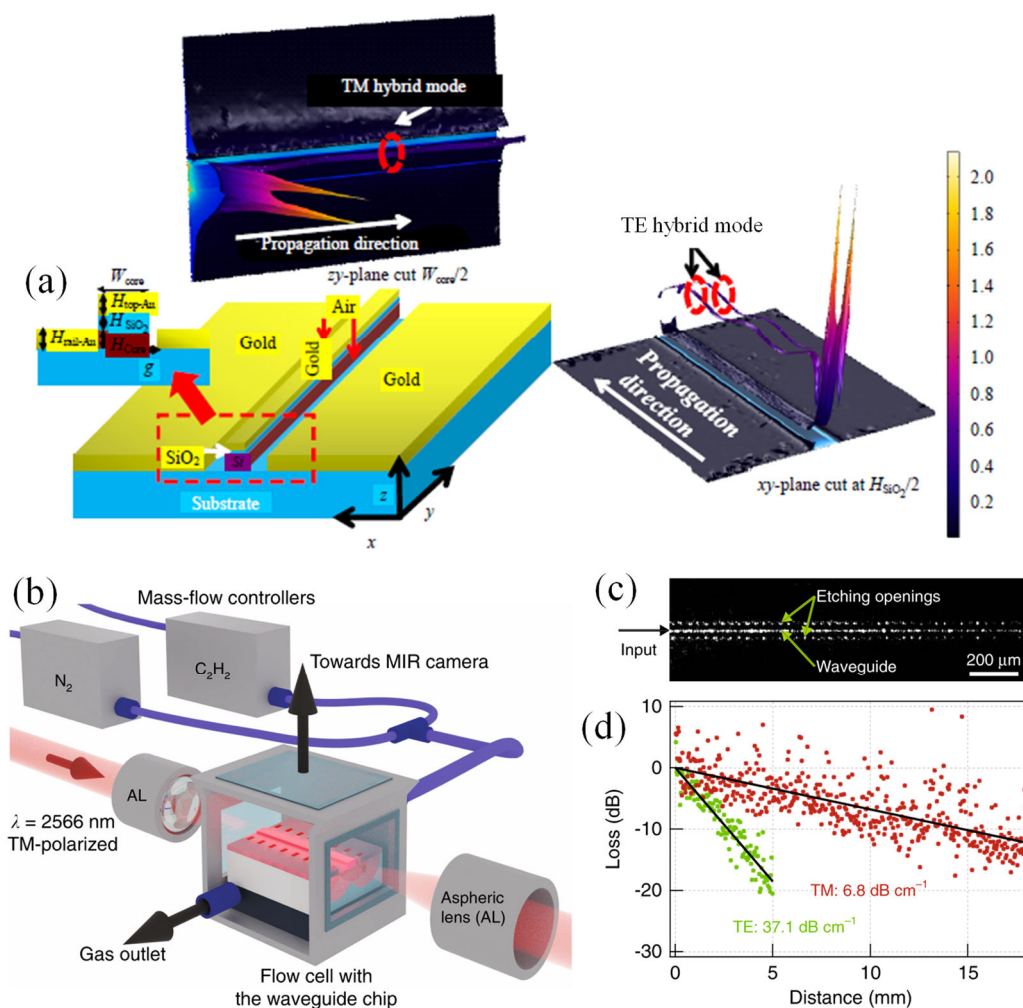


**Figure 4.** Schematic representation of a polarization-independent HPWG structure, (b) Outline of the experimental setup [67], (c) Top-view MIR image of the WG at 2566  $\mu\text{m}$ , showing the guided mode visible through out-of-plane scattering at WG roughness and imperfections [67], (d) Propagation loss determined from the decay of out-of-plane scattered light for both TM and TE polarizations. The TE mode, which is well confined in the Ta<sub>2</sub>O<sub>5</sub> membrane, experiences higher loss due to material absorption compared to the strongly delocalized TM mode [67].

#### 4.2. Gas Sensors based on the Mechanism of Wavelength Interrogation Method

Photonic sensors based on the wavelength interrogation method represent a cutting-edge approach to gas detection, capitalizing on the interplay between light and gas molecules. This method encompasses monitoring shifts in the wavelength of light as it passes through or interacts with a gas sample [13]. Functional polymers that are sensitive to gas absorption play a crucial role in the development of advanced photonic gas sensors. These polymers are designed to interact specifically with certain gas molecules, causing changes in their physical or chemical properties upon gas absorption. Such changes can include alterations in refractive index, optical absorption, or fluorescence properties, which can be precisely detected using photonic methods. Polymers like polyhexamethylene biguanide (PHMB) [13,57,80], [81,82], polyaniline (PANI) [83–85], polypyrrole (PPy) [86–88], and poly (ethylene oxide) (PEO) [89,90] have been extensively studied for their gas-sensitive properties. When integrated with photonic structures such as WGs or resonators, these polymers can significantly enhance the sensor's sensitivity and selectivity [53,58]. The gas-induced changes in the polymer can lead to detectable shifts in the light propagation characteristics within the photonic device. This interplay allows for real-time monitoring of gas concentrations with high accuracy. Moreover, functional polymers offer the advantage of tunability, where their chemical

structure can be modified to target specific gases, making them highly versatile for different sensing applications. Additionally, these polymers are often lightweight, cost-effective, and compatible with various substrates, facilitating their integration into compact and portable sensing platforms. Future research is focused on improving the stability and response time of these polymers, as well as exploring new polymer compositions and hybrid materials. Such advancements are expected to broaden the range of detectable gases and enhance the overall performance of photonic gas sensors, making them indispensable tools for environmental monitoring, industrial safety, and healthcare diagnostics.

Mi et al. reported a Si photonic refractometric CO<sub>2</sub> gas sensor capable of detecting CO<sub>2</sub> at atmospheric concentrations and operating at room temperature [82]. This sensor employed a PHMB polymer that undergoes a reversible change in refractive index upon absorbing and releasing CO<sub>2</sub> molecules, functioning independently of humidity (see Figure 5 (a)). The sensor's SEM image is depicted in Figure 5 (b). For the CO<sub>2</sub> sensing experiment, the chamber was preconditioned by flooding it with N<sub>2</sub> gas for 10 minutes. The initial resonance spectrum of the MRR, centered around the 1.55 μm wavelength, is displayed by the black curve in Figure 5 (c). This spectrum revealed a loaded quality factor (Q factor) of  $1.92 \times 10^4$  ( $\pm 2\%$ ) for the MRR. Subsequently, 0.5% CO<sub>2</sub> gas was introduced into the chamber, and the resonance spectrum was measured again after 2 minutes, once the sensor's response had stabilized. The presence of CO<sub>2</sub> gas resulted in the resonance spectrum shown by the red curve in Figure 5 (c), with a loaded Q factor of  $1.87 \times 10^4$  ( $\pm 2\%$ ), which matches the initial Q factor within experimental uncertainty. Thus, the two resonance spectra are nearly identical except for a small blue shift in the resonance wavelength. This shift indicates that CO<sub>2</sub> absorption reduces the refractive index of the PHMB polymer while having a minimal effect on optical absorption. This refractive index change is attributed to a redistribution of the electron density in the polymer's repeating units due to CO<sub>2</sub> molecule binding, altering its polarizability. The sensor detected CO<sub>2</sub> concentrations ranging from 0 to 500 ppm with a sensitivity of  $6 \times 10^{-9}$  RIU/ppm and a detection limit of 20 ppm. The MRR transducer offers a promising integrated solution for creating low-cost, compact CO<sub>2</sub> sensors, ideal for use in sensor networks for precise environmental monitoring of greenhouse gases [82].

A year later, Mi et al. introduced a Si photonic dual-gas sensor utilizing a wavelength-multiplexed MRR array for detecting both H<sub>2</sub> and CO<sub>2</sub> gases simultaneously [80]. The schematic of this dual-gas sensor, depicted in Figure 5 (d), features an array of three MRRs evanescently coupled to a single straight WG. The sensor was built on SOI substrate with a Si layer of 220 nm thickness on a 3 μm-thick SiO<sub>2</sub> layer. The WG, designed to be 450 nm wide, supports a single TE mode with an effective index ( $n_{\text{eff}}$ ) of 2.29 at the 1.55 μm wavelength. Microring 1, air-cladded, acts as a reference sensor to monitor temperature and laser power variations. Microrings 2 and 3 serve as sensors for H<sub>2</sub> and CO<sub>2</sub> gases respectively, functionalized with Pd and PHMB, as revealed in the cross-sectional diagrams in Figure 5 (e) and Figure 5 (f). The SEM image of the Pd-MRR is presented in Figure 5 (g). Figure 5 (h) shows the spectral response of the sensor chip after the test chamber was preconditioned by flooding it with N<sub>2</sub> gas for 10 minutes. The plot clearly shows three distinct resonances, each corresponding to one of the MRRs. Gas sensing experiments revealed that the PHMB-functionalized MRR was highly sensitive to CO<sub>2</sub> gas and had excellent selectivity against H<sub>2</sub>. Conversely, the Pd-functionalized MRR showed sensitivity to both H<sub>2</sub> and CO<sub>2</sub> gases, making it unsuitable for detecting H<sub>2</sub> in a CO<sub>2</sub>-containing gas mixture. The dual-gas sensing approach was shown to enable accurate measurement of H<sub>2</sub> concentration in the presence of CO<sub>2</sub> by compensating for the cross-sensitivity of Pd to CO<sub>2</sub>.

In a recent study, M.A. Butt conducted a numerical analysis on the loop-terminated Mach-Zehnder interferometer (LT-MZI) structure aimed at CO<sub>2</sub> gas detection applications (Refer to Figure 5 (i) [13]). The sensing arm was treated with a PHMB polymer, known for its high sensitivity and selectivity to CO<sub>2</sub> gas. When CO<sub>2</sub> gas was absorbed, it led to a reduction in the refractive index of the host material, which caused a shift in the interference pattern of the LT-MZI structure. This shift resulted in a redshift in the device's transmission spectrum, as illustrated in Figure 5 (j). The device demonstrated sensitivities of 7.63 pm/ppm, 34.46 pm/ppm, and 74.78 pm/ppm for sensing arm

lengths of 5  $\mu\text{m}$ , 10  $\mu\text{m}$ , and 15  $\mu\text{m}$ , respectively. Although increasing the sensitivity is possible, it would require a larger device size. This advanced sensor design enabled the detection of a wide range of  $\text{CO}_2$  gas concentrations from 0 to 524 ppm. The device, being both compact and highly sensitive, is a crucial tool for monitoring indoor  $\text{CO}_2$  levels, thereby fostering a healthier breathing environment for occupants.

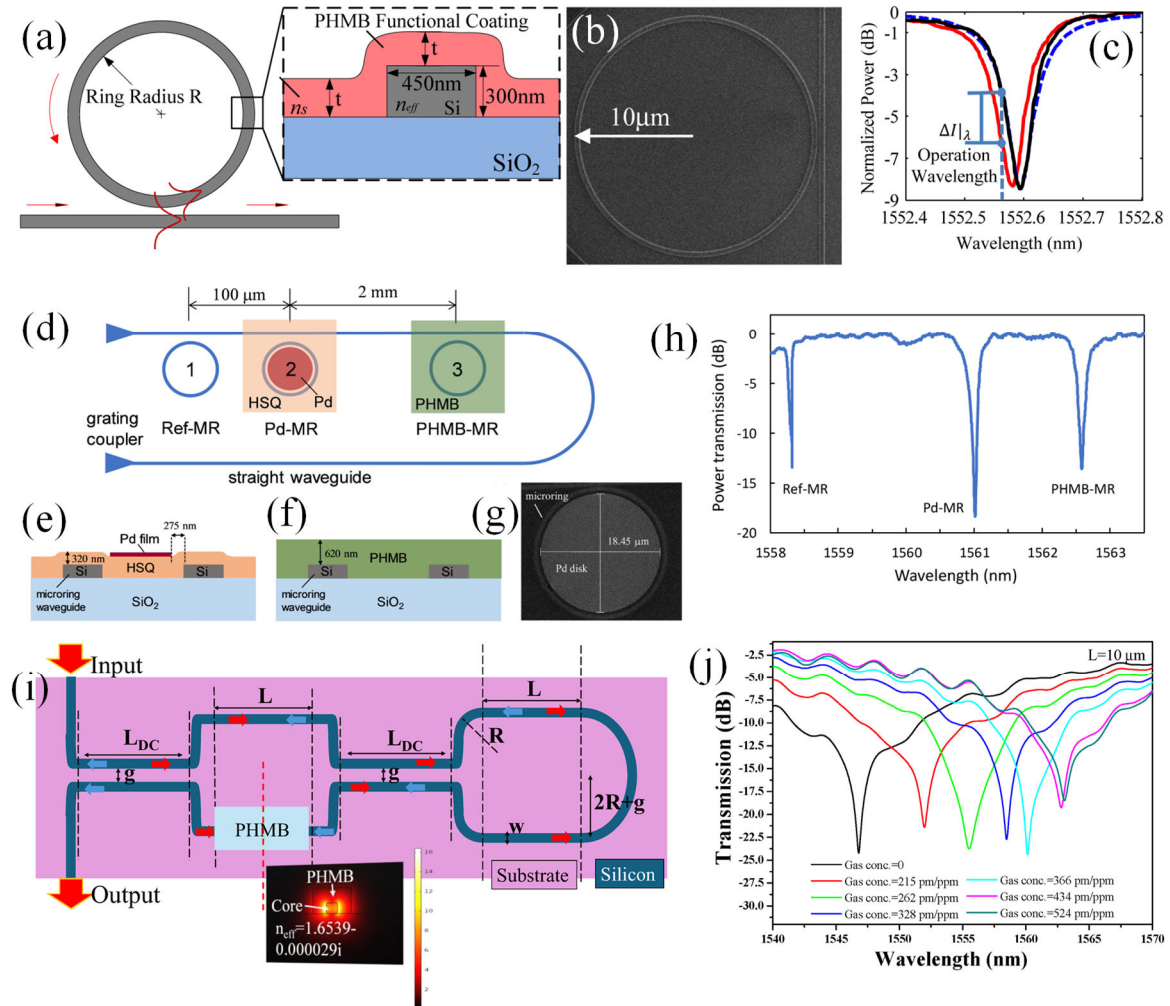


**Figure 5.** (a) Diagram of the Si MRR CO<sub>2</sub> gas sensor featuring a PHMB functional layer coating on the MRR WG [82], (b) SEM image of the Si MRR [82], (c) the measured resonance spectrum of the functionalized MRR is presented. The black curve represents the initial spectrum in pure N<sub>2</sub> gas, while the red curve shows the spectrum in the presence of a 0.5% CO<sub>2</sub> gas concentration. The blue dashed line indicates the resonance curve fit, which is used to correlate the transmitted powers to relative wavelength shifts [82], (d) Schematic representation of the dual-gas sensor, comprising an array of three MRRs: Ref-MR for reference, Pd-MR for H<sub>2</sub> sensing, and PHMB-MR for CO<sub>2</sub> sensing. Cross-sectional diagrams illustrating [80], (e) the Pd functional layer and (f) the PHMB coating [80], (g) SEM image of the Pd-MR, (h) Spectral response of the dual-gas sensor measured under N<sub>2</sub> gas flow conditions [80], (i) LT-MZI structure [13], (j) transmission spectrum of LT-MZI structure in the presence of varying CO<sub>2</sub> concentration [13].

## 5. Other Kinds of Photonic Gas Sensors

Apart from integrated photonic gas sensors, several other widely used photonic gas sensors are discussed in this section. These include metasurface (MS)-based gas sensors, optical fiber-based gas sensors, and photoacoustic spectroscopy (PAS) gas sensors. Each of these technologies leverages unique photonic principles to achieve high sensitivity and selectivity in gas detection. Together, these photonic gas sensor technologies are crucial in various applications, including environmental

monitoring, industrial safety, and medical diagnostics, pushing the boundaries of gas detection capabilities.

### 5.1. MS-Based Gas Sensors

MS-based gas sensors leverage engineered surfaces with sub-wavelength structures to manipulate light in novel ways, enhancing gas detection capabilities [91–93]. These MSs are composed of an array of nanostructures that can modify the phase, amplitude, and polarization of light, enabling highly sensitive and selective detection of gases [94,95]. The nanostructures can be designed to support resonant modes that enhance the interplay between light and gas molecules, thereby increasing the sensitivity of the sensor. When a gas molecule adsorbs by the functional polymers deposited onto the MS, it causes a measurable shift in the resonant frequency or intensity of the transmitted or reflected light, which can be correlated with the gas concentration [57,92]. MS-based gas sensors are advantageous due to their ultra-thin profiles, which allow for integration into compact devices, and their ability to operate across a wide range of wavelengths, including the visible and IR regions. These sensors are particularly useful for detecting trace amounts of gases in environmental monitoring, industrial process control, and medical diagnostics [96]. The flexibility in designing the nanostructures enables the tuning of the sensor's response to specific gases, providing high selectivity and sensitivity [97]. Additionally, progresses in assembly methods, such as electron beam lithography (EBL) and nanoimprint lithography (NIL), have facilitated the mass production of MS-based sensors, making them a promising technology for widespread gas sensing applications [98].

### 5.2. Optical Fiber-Based Gas Sensors

Optical fiber-based gas sensors utilize the properties of light transmission through optical fibers to detect and measure gas concentrations [15]. These sensors operate on various principles, including absorption spectroscopy, fluorescence, and surface plasmon resonance (SPR). In absorption spectroscopy-based optical fiber sensors, light transmitted through or along a gas-sensitive fiber segment is attenuated at specific wavelengths where the gas absorbs light [99,100]. This attenuation is used to determine the gas concentration. Fluorescence-based sensors involve the interplay of the target gas with a fluorescent material coated on or incorporated into the fiber [101–103]. The gas-induced changes in fluorescence intensity or wavelength shift are measured to quantify the gas concentration [104,105]. SPR-based optical fiber sensors employ a metal-coated fiber where the interplay of light with the metal surface excites surface plasmons, which are sensitive to changes in the refractive index near the fiber surface caused by gas adsorption [106,107]. Optical fiber sensors are highly sensitive, offer real-time monitoring, and can be deployed in harsh environments due to their robustness and resistance to electromagnetic interference. They are widely used in applications such as industrial safety monitoring, environmental pollution detection, and medical diagnostics. The ability to perform remote sensing and multiplexing, where multiple sensors are integrated into a single fiber, further enhances their utility in various gas sensing scenarios [108,109].

### 5.3. Photoacoustic Spectroscopy (PAS) Gas Sensors

Photoacoustic spectroscopy (PAS) gas sensors exploit the photoacoustic effect to detect gas concentrations with high sensitivity and selectivity [110,111]. In PAS, modulated light is absorbed by gas molecules, causing periodic heating and cooling, which generates pressure waves or acoustic signals. These pressure waves are detected by highly sensitive microphones or quartz tuning forks. The amplitude of the acoustic signal is proportional to the gas concentration, allowing for precise quantification of trace gases. PAS sensors can operate across a wide range of wavelengths, from UV to IR, making them versatile for detecting various gases [112–114]. The key advantages of PAS sensors include their ability to provide real-time measurements, their high sensitivity, which can reach parts-per-billion (ppb) levels, and their minimal interference from other gases, as the detection is based on the unique absorption characteristics of the target gas [115]. PAS technology is particularly effective

in detecting gases such as CO<sub>2</sub>, CH<sub>4</sub>, and VOCs. The development of compact, portable PAS sensors has expanded their use in field applications, providing a powerful tool for on-site gas analysis [116]. Advances in laser technology, such as the use of quantum cascade lasers (QCLs) [116], have further enhanced the sensitivity and selectivity of PAS sensors, making them an indispensable technology for modern gas sensing [117].

## 6. Fabrication Methods of Integrated Photonic Sensors

The fabrication of integrated photonic devices, including sensors, involves several sophisticated techniques that enable the miniaturization and integration of optical components onto a single chip [118]. These methods leverage advancements in materials science, nanotechnology, and semiconductor processing to create devices that can manipulate light with high precision and efficiency. One of the primary methods used in the fabrication of integrated photonic devices is photolithography [119]. This process involves transferring a geometric pattern from a photomask to a light-sensitive chemical photoresist layer on the substrate. The exposed areas of the photoresist are then developed, revealing the underlying substrate, which can be etched away to create the desired structures. Photolithography can produce features with dimensions in the order of nanometers, essential for the intricate designs required in photonic circuits.

Another critical fabrication technique is chemical vapor deposition (CVD). CVD is used to deposit thin films of materials, such as SiO<sub>2</sub> or SiN, which are essential for the WGs that channel light in photonic devices [120]. In this process, gaseous precursors react on the substrate surface to form a solid film. Variations of CVD, such as plasma-enhanced CVD (PECVD), can offer better control over film properties and deposition conditions, which is crucial for achieving high-quality optical components. Techniques such as atomic layer deposition (ALD) and molecular beam epitaxy (MBE) are used for the precise deposition of ultra-thin films and the growth of high-quality crystalline layers, respectively [121]. ALD allows for the deposition of conformal layers with atomic-level control, which is beneficial for creating multilayer structures and coatings with precise thicknesses [120]. MBE is used to grow epitaxial layers of materials, often with tailored electronic and optical properties, which are critical for the performance of photonic devices.

Alternatively, sol-gel method combined with dip-coating processes offers a promising avenue for the development of low-cost photonic sensors [122]. The sol-gel technique involves the synthesis of inorganic materials from molecular precursors, typically metal alkoxides, via a solution-based route. This method allows for precise control over material composition, structure, and morphology, facilitating the customization of sensor properties. By employing dip-coating, thin films of the synthesized sol-gel materials can be uniformly deposited onto substrates, enabling the fabrication of sensor coatings with tailored thickness and optical characteristics. This approach not only minimizes material wastage but also reduces production costs associated with traditional deposition techniques. Furthermore, the simplicity and scalability of sol-gel processing make it accessible for mass production, contributing to the affordability of photonic sensors without compromising performance [123].

Electron beam lithography (EBL) is another advanced method utilized in the fabrication of integrated photonic devices [124,125]. Unlike photolithography, which uses light to transfer patterns, EBL uses a focused beam of electrons. This technique allows for even finer patterning and is particularly useful for creating nanoscale features that are beyond the resolution limits of traditional photolithography. EBL is often used for prototyping and fabricating complex photonic structures like photonic crystals and metamaterials. Etching processes, including both dry etching (such as reactive ion etching (RIE)) and wet etching, are employed to remove material and define the final geometry of the photonic devices [126,127]. Dry etching uses plasma to etch away material in a highly controlled manner, allowing for anisotropic etching profiles essential for vertical sidewalls in WGs. Wet etching, on the other hand, uses liquid chemicals to selectively dissolve materials, which can be more suitable for certain materials and applications.

## 7. Challenges and Prospects

Integrated photonic gas sensors represent a promising frontier in gas sensing technology, leveraging the advantages of photonics to achieve high sensitivity, selectivity, and miniaturization. These sensors integrate photonic circuits on a single chip to detect and measure gas concentrations, using light-matter interactions. However, despite their potential, several challenges need to be addressed to realize their full capabilities and widespread adoption. The selectivity of photonic gas sensors poses significant challenges in their practical implementation. One primary concern is the interference from other gases present in the environment, which can lead to false readings or inaccurate detection. Achieving high selectivity requires sensor designs that can discriminate between target gases and potential interferents effectively. Additionally, variations in environmental conditions such as temperature and humidity can further complicate selectivity, as they may influence the sensor's response to different gases. Developing robust algorithms for signal processing and pattern recognition is essential to enhance the selectivity of photonic gas sensors, enabling reliable and accurate detection in real-world applications.

Another major concern is the fabrication and integration complexity. Creating integrated photonic circuits that can precisely and reliably detect gases requires advanced manufacturing techniques, often involving sophisticated lithography and material deposition processes [128]. Ensuring consistent quality and performance across large-scale production adds another layer of difficulty. Additionally, integrating various components, such as light sources, WGs, detectors, and gas-sensitive materials, into a single compact device without compromising performance remains a significant engineering challenge. Another critical issue is the sensitivity and selectivity of the sensors. While photonic gas sensors can achieve high sensitivity due to their interaction with light, distinguishing between different gas species accurately can be problematic [129]. This is because many gases may exhibit similar optical absorption features, leading to cross-sensitivity and potential false readings [130]. Developing materials and sensor designs that enhance selectivity, possibly using functionalized surfaces or advanced signal processing algorithms, is essential to overcome this challenge [131].

Ensuring the stability of photonic gas sensors is crucial for their reliable and long-term operation. One significant issue is the drift in sensor response over time, which can result from factors such as aging of sensor materials, variations in manufacturing processes, and exposure to environmental conditions. Drift can lead to a decrease in sensor accuracy and sensitivity, impacting the reliability of gas detection. Maintaining stability often requires careful calibration and periodic recalibration of the sensor to correct for any deviations in its response. Furthermore, efforts to enhance the stability of photonic gas sensors may involve the use of robust materials, protective coatings, and advanced encapsulation techniques to minimize the effects of environmental factors and ensure consistent performance over extended periods.

The limit of detection (LOD) presents a critical challenge for photonic gas sensors, influencing their effectiveness in detecting trace amounts of target gases. Achieving low LODs is essential, particularly in applications where detecting very low concentrations of gases is necessary for safety or environmental monitoring. However, several factors can limit the LOD of photonic gas sensors, including inherent noise in the sensor system, background interference from other gases, and limitations in the sensor's sensitivity and dynamic range. Improving the LOD often involves optimizing sensor design parameters, such as the selection of appropriate sensing materials, enhancing signal-to-noise ratios through advanced signal processing techniques, and minimizing cross-sensitivity to non-target gases [132]. Additionally, advancements in nanotechnology and materials science have opened new avenues for enhancing the sensitivity and selectivity of photonic gas sensors, potentially pushing the LOD to even lower levels [133].

Despite these obstacles, the prospects for integrated photonic gas sensors are promising. Advances in material science, such as the development of novel nanomaterials and metamaterials, offer pathways to enhance sensor performance [91,92,96], [97,134]. These materials can be engineered to have specific interactions with certain gas molecules, improving both sensitivity and selectivity. Moreover, the integration of photonic sensors with complementary technologies, such as

microelectromechanical systems (MEMS) and microfluidics, can lead to the development of multifunctional sensing platforms that are compact, robust, and capable of real-time monitoring.

In terms of applications, integrated photonic gas sensors have the potential to revolutionize fields such as environmental monitoring, industrial process control, and healthcare [80]. For instance, they could provide real-time, on-site monitoring of air quality with unprecedented precision, helping to address environmental and public health concerns [135]. In industrial settings, these sensors could be used for the continuous monitoring of hazardous gases, improving safety and operational efficiency. In healthcare, they could enable non-invasive diagnostics through the detection of biomarkers in breath, offering a new avenue for early disease detection.

## 8. Concluding Remarks

Gas sensing plays a vital role in ensuring safety and prevention by detecting harmful gases before they reach dangerous levels. In industrial settings, gas sensors can identify leaks of toxic or flammable gases, preventing explosions and protecting workers from poisoning. In homes and commercial buildings, they can detect carbon monoxide, providing early warnings that prevent fatalities. Additionally, gas sensing is critical in disaster prevention, such as detecting methane leaks in mining operations to avert explosions. By providing real-time monitoring and alerts, gas sensing technologies significantly enhance safety and prevent accidents in various environments. Integrated photonic gas sensors have demonstrated significant advancements in sensitivity, selectivity, and miniaturization, offering a robust platform for real-time and on-site gas detection. These sensors leverage the principles of photonic integration to enhance performance and reduce the size and cost of traditional gas sensing systems.

The successful integration of various photonic components on a single chip has enabled the detection of multiple gases simultaneously with high precision. Looking forward, the future of integrated photonic gas sensors is promising, with ongoing research focused on further enhancing their sensitivity, expanding their detection range, and improving their robustness in diverse environmental conditions. Advances in materials science, nanofabrication techniques, and data processing algorithms are expected to play crucial roles in these developments. Additionally, the integration of these sensors with the Internet of Things (IoT) could revolutionize environmental monitoring, industrial safety, and healthcare applications by providing continuous, real-time monitoring and analysis of gas compositions.

**Author Contributions:** Conceptualization, M.A.B.; methodology, M.A.B.; software, M.A.B.; validation, M.A.B. and R.P.; formal analysis, M.A.B.; investigation, M.A.B.; resources, R.P.; data curation, M.A.B.; writing—original draft preparation, M.A.B.; writing—review and editing, M.A.B. and R.P.; visualization, M.A.B.; supervision, R.P.; project administration, R.P.; funding acquisition, M.A.B. All authors have read and agreed to the published version of the manuscript.

**Funding:** This research received no external funding.

**Institutional Review Board Statement:** Not applicable.

**Informed Consent Statement:** Not applicable.

**Data Availability Statement:** Not applicable.

**Acknowledgments:** The author acknowledges the constant support of Warsaw University of Technology in the completion of this work.

**Conflicts of Interest:** The authors declare no conflicts of interest.

## References

1. J. Wang, S. Viciano-Tudela, L. Parra, R. Lacuesta, and J. Lloret, 'Evaluation of Suitability of Low-Cost Gas Sensors for Monitoring Indoor and Outdoor Urban Areas', *IEEE Sens. J.*, vol. 23, no. 18, pp. 20968–20975, Sep. 2023, doi: 10.1109/JSEN.2023.3301651.
2. L. Yang *et al.*, 'Moisture-resistant, stretchable NO<sub>x</sub> gas sensors based on laser-induced graphene for environmental monitoring and breath analysis', *Microsyst. Nanoeng.*, vol. 8, no. 1, pp. 1–12, Jul. 2022, doi: 10.1038/s41378-022-00414-x.

3. J. Lee *et al.*, 'High-performance gas sensor array for indoor air quality monitoring: the role of Au nanoparticles on WO<sub>3</sub>, SnO<sub>2</sub>, and NiO-based gas sensors', *J. Mater. Chem. A*, vol. 9, no. 2, pp. 1159–1167, Jan. 2021, doi: 10.1039/D0TA08743B.
4. 'Recent Development of Gas Sensing Platforms Based on 2D Atomic Crystals | Research'. Accessed: Jun. 06, 2024. [Online]. Available: <https://spj.science.org/doi/10.34133/2021/9863038>
5. 'Sensors | Free Full-Text | The Challenges of Prolonged Gas Sensing in the Modern Urban Environment'. Accessed: Jun. 06, 2024. [Online]. Available: <https://www.mdpi.com/1424-8220/20/18/5189>
6. U. Yaqoob and M. I. Younis, 'Chemical Gas Sensors: Recent Developments, Challenges, and the Potential of Machine Learning—A Review', *Sensors*, vol. 21, no. 8, Art. no. 8, Jan. 2021, doi: 10.3390/s21082877.
7. X. Liu, S. Cheng, H. Liu, S. Hu, D. Zhang, and H. Ning, 'A Survey on Gas Sensing Technology', *Sensors*, vol. 12, no. 7, Art. no. 7, Jul. 2012, doi: 10.3390/s120709635.
8. M. N. Padvi, A. V. Moholkar, S. R. Prasad, and N.R.Prasad, 'A Critical Review on Design and Development of Gas Sensing Materials', *Eng. Sci.*, vol. Volume 15 (September 2021), no. 0, pp. 20–37, Mar. 2021.
9. G. Eranna, B. C. Joshi, D. P. Runthala, and R. P. Gupta, 'Oxide Materials for Development of Integrated Gas Sensors—A Comprehensive Review', *Crit. Rev. Solid State Mater. Sci.*, vol. 29, no. 3–4, pp. 111–188, Jul. 2004, doi: 10.1080/10408430490888977.
10. S. Dhall, B. R. Mehta, A. K. Tyagi, and K. Sood, 'A review on environmental gas sensors: Materials and technologies', *Sens. Int.*, vol. 2, p. 100116, Jan. 2021, doi: 10.1016/j.sintl.2021.100116.
11. M. M. Ariannejad, E. Akbari, and E. Hanafi, 'Silicon sub-wavelength grating resonator structures for gas sensor', *Superlattices Microstruct.*, vol. 142, p. 106506, Jun. 2020, doi: 10.1016/j.spmi.2020.106506.
12. 'Micromachines | Free Full-Text | Breakthrough in Silicon Photonics Technology in Telecommunications, Biosensing, and Gas Sensing'. Accessed: Jun. 07, 2024. [Online]. Available: <https://www.mdpi.com/2072-666X/14/8/1637>
13. M. A. Butt, 'Loop-Terminated Mach-Zehnder Interferometer Integrated with Functional Polymer for CO<sub>2</sub> Gas Sensing'. Preprints, May 28, 2024. doi: 10.20944/preprints202405.1850.v1.
14. A. Aksnes, 'Photonic Sensors for Health and Environmental Monitoring', in *Sensors for Environment, Health and Security*, M.-I. Baraton, Ed., Dordrecht: Springer Netherlands, 2009, pp. 191–203. doi: 10.1007/978-1-4020-9009-7\_12.
15. M. A. Butt, G. S. Voronkov, E. P. Grakhova, R. V. Kutluyarov, N. L. Kazanskiy, and S. N. Khonina, 'Environmental Monitoring: A Comprehensive Review on Optical Waveguide and Fiber-Based Sensors', *Biosensors*, vol. 12, no. 11, Art. no. 11, Nov. 2022, doi: 10.3390/bios12111038.
16. A. De and D. Kalita, 'Bio-Fabricated Gold and Silver Nanoparticle Based Plasmonic Sensors for Detection of Environmental Pollutants: An Overview', *Crit. Rev. Anal. Chem.*, vol. 53, no. 3, pp. 672–688, Apr. 2023, doi: 10.1080/10408347.2021.1970507.
17. J. Zhou *et al.*, 'Detection of volatile organic compounds using mid-infrared silicon nitride waveguide sensors', *Sci. Rep.*, vol. 12, no. 1, Art. no. 1, Apr. 2022, doi: 10.1038/s41598-022-09597-9.
18. M. A. Butt, S. A. Degtyarev, S. N. Khonina, and N. L. Kazanskiy, 'An evanescent field absorption gas sensor at mid-IR 3.39  $\mu\text{m}$  wavelength', *J. Mod. Opt.*, vol. 64, no. 18, pp. 1892–1897, Oct. 2017, doi: 10.1080/09500340.2017.1325947.
19. J. J. Rose *et al.*, 'Carbon Monoxide Poisoning: Pathogenesis, Management, and Future Directions of Therapy', *Am. J. Respir. Crit. Care Med.*, vol. 195, no. 5, pp. 596–606, Mar. 2017, doi: 10.1164/rccm.201606-1275CI.
20. L. T. N. Ngoc, D. Park, and Y.-C. Lee, 'Human Health Impacts of Residential Radon Exposure: Updated Systematic Review and Meta-Analysis of Case-Control Studies', *Int. J. Environ. Res. Public Health*, vol. 20, no. 1, Art. no. 1, Jan. 2023, doi: 10.3390/ijerph20010097.
21. 'IJERPH | Free Full-Text | Volatile Organic Compounds (VOCs) as Environmental Pollutants: Occurrence and Mitigation Using Nanomaterials'. Accessed: Jun. 08, 2024. [Online]. Available: <https://www.mdpi.com/1660-4601/18/24/13147>
22. W. H. Peterson, R. H. Burris, R. Sant, and H. N. Little, 'Toxic Gases in Silage, Production of Toxic Gas (Nitrogen Oxides) in Silage Making', *J. Agric. Food Chem.*, vol. 6, no. 2, pp. 121–126, Feb. 1958, doi: 10.1021/jf60084a006.
23. R. P. Pangenji, B. Timilsina, P. R. Oli, S. Khadka, and P. R. Regmi, 'A multidisciplinary approach to accidental inhalational ammonia injury: A case report', *Ann. Med. Surg.*, vol. 82, p. 104741, Oct. 2022, doi: 10.1016/j.amsu.2022.104741.
24. 'Ozone as Janus: this controversial gas can be either toxic or medically useful - Bocci - 2004 - Mediators of Inflammation - Wiley Online Library'. Accessed: Jun. 08, 2024. [Online]. Available: <https://onlinelibrary.wiley.com/doi/10.1080/0962935062000197083>
25. X. Zhou, X. Zhou, C. Wang, and H. Zhou, 'Environmental and human health impacts of volatile organic compounds: A perspective review', *Chemosphere*, vol. 313, p. 137489, Feb. 2023, doi: 10.1016/j.chemosphere.2022.137489.

26. J. Jiang *et al.*, 'Hydrogen Sulfide—Mechanisms of Toxicity and Development of an Antidote', *Sci. Rep.*, vol. 6, no. 1, p. 20831, Feb. 2016, doi: 10.1038/srep20831.
27. N. S. Anjana, A. Amarnath, and M. V. Harindranathan Nair, 'Toxic hazards of ammonia release and population vulnerability assessment using geographical information system', *J. Environ. Manage.*, vol. 210, pp. 201–209, Mar. 2018, doi: 10.1016/j.jenvman.2018.01.021.
28. W. F. Ho, H. P. Chan, and K. L. Yang, 'Planar Optical Waveguide Platform for Gas Sensing Using Liquid Crystal', *IEEE Sens. J.*, vol. 13, no. 7, pp. 2521–2522, Jul. 2013, doi: 10.1109/JSEN.2013.2254596.
29. I. Vitoria, E. E. Gallego, S. Melendi-Espina, M. Hernaez, C. Ruiz Zamarreño, and I. R. Matías, 'Gas Sensor Based on Lossy Mode Resonances by Means of Thin Graphene Oxide Films Fabricated onto Planar Coverslips', *Sensors*, vol. 23, no. 3, Art. no. 3, Jan. 2023, doi: 10.3390/s23031459.
30. L. Zheng, N. Keppler, H. Zhang, P. Behrens, and B. Roth, 'Planar Polymer Optical Waveguide with Metal-Organic Framework Coating for Carbon Dioxide Sensing', *Adv. Mater. Technol.*, vol. 7, no. 12, p. 2200395, 2022, doi: 10.1002/admt.202200395.
31. I. Dominguez, I. Del Villar, O. Fuentes, J. M. Corres, and I. R. Matias, 'Dually nanocoated planar waveguides towards multi-parameter sensing', *Sci. Rep.*, vol. 11, no. 1, p. 3669, Feb. 2021, doi: 10.1038/s41598-021-83324-8.
32. C. A. Barrios *et al.*, 'Label-free optical biosensing with slot-waveguides', *Opt. Lett.*, vol. 33, no. 7, pp. 708–710, Apr. 2008, doi: 10.1364/OL.33.000708.
33. M. A. Butt and R. Piramidowicz, 'Standard slot waveguide and double hybrid plasmonic waveguide configurations for enhanced evanescent field absorption methane gas sensing', *Photonics Lett. Pol.*, vol. 14, no. 1, Art. no. 1, Mar. 2022, doi: 10.4302/plp.v14i1.1121.
34. V. M. N. Passaro, F. Dell'Olio, C. Ciminelli, and M. N. Armenise, 'Efficient Chemical Sensing by Coupled Slot SOI Waveguides', *Sensors*, vol. 9, no. 2, Art. no. 2, Feb. 2009, doi: 10.3390/s90201012.
35. C. A. Barrios, 'Optical Slot-Waveguide Based Biochemical Sensors', *Sensors*, vol. 9, no. 6, pp. 4751–4765, 2009, doi: 10.3390/s90604751.
36. C. Ranacher, C. Consani, R. Jannesari, T. Grille, and B. Jakoby, 'Numerical Investigations of Infrared Slot Waveguides for Gas Sensing', *Proceedings*, vol. 2, no. 13, Art. no. 13, 2018, doi: 10.3390/proceedings2130799.
37. L. Torrijos-Morán, A. Griol, and J. García-Rupérez, 'Experimental study of subwavelength grating bimodal waveguides as ultrasensitive interferometric sensors', *Opt. Lett.*, vol. 44, no. 19, pp. 4702–4705, Oct. 2019, doi: 10.1364/OL.44.004702.
38. K. Awasthi, N. Malviya, and A. Kumar, 'Silicon Subwavelength Grating Slot Waveguide based Optical Sensor for Label Free Detection of Fluoride Ion in Water', *IETE Tech. Rev.*, vol. 0, no. 0, pp. 1–12, 2023, doi: 10.1080/02564602.2023.2246429.
39. N. L. Kazanskiy, S. N. Khonina, and M. A. Butt, 'Subwavelength Grating Double Slot Waveguide Racetrack Ring Resonator for Refractive Index Sensing Application', *Sensors*, vol. 20, no. 12, Art. no. 12, Jan. 2020, doi: 10.3390/s20123416.
40. Z. Tu, D. Gao, M. Zhang, and D. Zhang, 'High-sensitivity complex refractive index sensing based on Fano resonance in the subwavelength grating waveguide micro-ring resonator', *Opt. Express*, vol. 25, no. 17, pp. 20911–20922, Aug. 2017, doi: 10.1364/OE.25.020911.
41. K. E. Arledge, B. Uchoa, Y. Zou, and B. Weng, 'Topological sensing with photonic arrays of resonant circular waveguides', *Phys. Rev. Res.*, vol. 3, no. 3, p. 033106, Jul. 2021, doi: 10.1103/PhysRevResearch.3.033106.
42. G. Si, E. J. Teo, A. A. Bettiol, J. Teng, and A. J. Danner, 'Suspended slab and photonic crystal waveguides in lithium niobate', *J. Vac. Sci. Technol. B*, vol. 28, no. 2, pp. 316–320, Mar. 2010, doi: 10.1116/1.3327925.
43. M. A. Butt, S. N. Khonina, and N. L. Kazanskiy, 'Recent advances in photonic crystal optical devices: A review', *Opt. Laser Technol.*, vol. 142, p. 107265, Oct. 2021, doi: 10.1016/j.optlastec.2021.107265.
44. L. Kassa-Baghdouche and E. Cassan, 'Sensitivity analysis of ring-shaped slotted photonic crystal waveguides for mid-infrared refractive index sensing', *Opt. Quantum Electron.*, vol. 51, no. 10, p. 328, Sep. 2019, doi: 10.1007/s11082-019-2040-4.
45. A. Rostamian, J. Midkiff, K. M. Yoo, Y. Cheng, S. Chakravarty, and R. Chen, 'Mid-Infrared Trace Gas Sensing Using Photonic Crystal Waveguides', in *2019 IEEE Photonics Society Summer Topical Meeting Series (SUM)*, Ft. Lauderdale, FL, USA: IEEE, Jul. 2019, pp. 1–2. doi: 10.1109/PHOSST.2019.8795083.
46. Z. Peng *et al.*, 'Slow-light-enhanced on-chip 1D and 2D photonic crystal waveguide gas sensing in near-IR with an ultrahigh interaction factor', *Photonics Res.*, vol. 11, no. 10, pp. 1647–1656, Oct. 2023, doi: 10.1364/PRJ.494762.
47. A. K. Goyal and S. Pal, 'Design and simulation of high sensitive photonic crystal waveguide sensor', *Optik*, vol. 126, no. 2, pp. 240–243, Jan. 2015, doi: 10.1016/j.ijleo.2014.08.174.
48. M. A. Butt and N. L. Kazansky, 'SOI Suspended membrane waveguide at 3.39  $\mu\text{m}$  for gas sensing application', *Photonics Lett. Pol.*, vol. 12, no. 2, Art. no. 2, Jul. 2020, doi: 10.4302/plp.v12i2.1034.

49. M. Vlk, A. Datta, S. Alberti, G. S. Murugan, A. Aksnes, and J. Jágerská, 'Free-standing tantalum pentoxide waveguides for gas sensing in the mid-infrared', *Opt. Mater. Express*, vol. 11, no. 9, pp. 3111–3124, Sep. 2021, doi: 10.1364/OME.430994.
50. K. M. Yoo, J. Midkiff, A. Rostamian, S. Chakravarty, and R. T. Chen, 'Suspended Membrane InGaAs Photonic Crystal Waveguides for ammonia sensing at  $\lambda=6.15\mu\text{m}$ ', in *Conference on Lasers and Electro-Optics (2019)*, paper STh1F.6, Optica Publishing Group, May 2019, p. STh1F.6. doi: 10.1364/CLEO\_SI.2019.STh1F.6.
51. K. M. Yoo, J. Midkiff, A. Rostamian, C. Chung, H. Dalir, and R. T. Chen, 'InGaAs Membrane Waveguide: A Promising Platform for Monolithic Integrated Mid-Infrared Optical Gas Sensor', *ACS Sens.*, vol. 5, no. 3, pp. 861–869, Mar. 2020, doi: 10.1021/acssensors.0c00180.
52. Y. Xu, F. Wang, Y. Gao, D. Zhang, X. Sun, and P. Berini, 'Straight Long-Range Surface Plasmon Polariton Waveguide Sensor Operating at  $\lambda_0 = 850 \text{ nm}$ ', *Sensors*, vol. 20, no. 9, Art. no. 9, Jan. 2020, doi: 10.3390/s20092507.
53. S. N. Khonina, N. L. Kazanskiy, M. A. Butt, A. Kaźmierczak, and R. Piramidowicz, 'Plasmonic sensor based on metal-insulator-metal waveguide square ring cavity filled with functional material for the detection of CO<sub>2</sub> gas', *Opt. Express*, vol. 29, no. 11, pp. 16584–16594, May 2021, doi: 10.1364/OE.423141.
54. M. A. Butt, S. N. Khonina, and N. L. Kazanskiy, 'Plasmonics: A Necessity in the Field of Sensing-A Review (Invited)', *Fiber Integr. Opt.*, vol. 40, no. 1, pp. 14–47, Jan. 2021, doi: 10.1080/01468030.2021.1902590.
55. N. L. Kazanskiy, S. N. Khonina, and M. A. Butt, 'Plasmonic sensors based on Metal-insulator-metal waveguides for refractive index sensing applications: A brief review', *Phys. E Low-Dimens. Syst. Nanostructures*, vol. 117, p. 113798, Mar. 2020, doi: 10.1016/j.physe.2019.113798.
56. M. A. Butt, M. Shahbaz, and R. Piramidowicz, 'Racetrack Ring Resonator Integrated with Multimode Interferometer Structure Based on Low-Cost Silica-Titania Platform for Refractive Index Sensing Application', *Photonics*, vol. 10, no. 9, Art. no. 9, Sep. 2023, doi: 10.3390/photonics10090978.
57. N. L. Kazanskiy, M. A. Butt, and S. N. Khonina, 'Carbon Dioxide Gas Sensor Based on Polyhexamethylene Biguanide Polymer Deposited on Silicon Nano-Cylinders Metasurface', *Sensors*, vol. 21, no. 2, Art. no. 2, Jan. 2021, doi: 10.3390/s21020378.
58. M. A. Butt, N. L. Kazanskiy, and S. N. Khonina, 'On-chip symmetrically and asymmetrically transformed plasmonic Bragg grating formation loaded with a functional polymer for filtering and CO<sub>2</sub> gas sensing applications', *Measurement*, vol. 201, p. 111694, Sep. 2022, doi: 10.1016/j.measurement.2022.111694.
59. 'Optical Fiber Fabry-Perot Interferometric CO<sub>2</sub> Gas Sensor Using Guanidine Derivative Polymer Functionalized Layer | IEEE Journals & Magazine | IEEE Xplore'. Accessed: May 04, 2024. [Online]. Available: <https://ieeexplore.ieee.org/document/8249792/>
60. N. L. Kazanskiy, S. N. Khonina, and M. A. Butt, 'Advancement in Silicon Integrated Photonics Technologies for Sensing Applications in Near-Infrared and Mid-Infrared Region: A Review', *Photonics*, vol. 9, no. 5, Art. no. 5, May 2022, doi: 10.3390/photonics9050331.
61. Y. Song, B. Li, H. Zhang, M. Li, Q. Li, and J.-J. He, 'Silicon Waveguide Sensors for Carbon Dioxide Gas Sensing in the Mid-Infrared Region', *Photonics*, vol. 10, no. 2, Art. no. 2, Feb. 2023, doi: 10.3390/photonics10020120.
62. M. A. Butt, 'Dielectric Waveguide-Based Sensors with Enhanced Evanescent Field: Unveiling the Dynamic Interaction with the Ambient Medium for Biosensing and Gas-Sensing Applications – A Review', *Photonics*, vol. 11, no. 3, Art. no. 3, Mar. 2024, doi: 10.3390/photonics11030198.
63. S. N. Khonina, N. L. Kazanskiy, and M. A. Butt, 'Evanescent Field Ratio Enhancement of a Modified Ridge Waveguide Structure for Methane Gas Sensing Application', *IEEE Sens. J.*, vol. 20, no. 15, pp. 8469–8476, Aug. 2020, doi: 10.1109/JSEN.2020.2985840.
64. C. Consani, C. Ranacher, A. Tortschanoff, T. Grille, P. Irsigler, and B. Jakoby, 'Evanescent-Wave Gas Sensing Using an Integrated Thermal Light Source', *Proceedings*, vol. 1, no. 4, Art. no. 4, 2017, doi: 10.3390/proceedings1040550.
65. M. A. Butt, S. N. Khonina, and N. L. Kazanskiy, 'Enhancement of evanescent field ratio in a silicon strip waveguide by incorporating a thin metal film', *Laser Phys.*, vol. 29, no. 7, p. 076202, May 2019, doi: 10.1088/1555-6611/ab1414.
66. V. Chandra and R. Ranjan, 'Performance analysis of different slot waveguide structures for evanescent field based gas sensor applications', *Opt. Quantum Electron.*, vol. 53, no. 8, p. 457, Aug. 2021, doi: 10.1007/s11082-021-03102-8.
67. M. Vlk *et al.*, 'Extraordinary evanescent field confinement waveguide sensor for mid-infrared trace gas spectroscopy', *Light Sci. Appl.*, vol. 10, no. 1, Art. no. 1, Jan. 2021, doi: 10.1038/s41377-021-00470-4.
68. C. Ranacher *et al.*, 'Characterization of Evanescent Field Gas Sensor Structures Based on Silicon Photonics', *IEEE Photonics J.*, vol. 10, no. 5, pp. 1–14, Oct. 2018, doi: 10.1109/JPHOT.2018.2866628.
69. 'Ultrasensitive Indium Phosphide Nanomembrane Wearable Gas Sensors - Wei - ENERGY & ENVIRONMENTAL MATERIALS - Wiley Online Library'. Accessed: Jun. 07, 2024. [Online]. Available: <https://onlinelibrary.wiley.com/doi/full/10.1002/eem2.12763>

70. V. Rosborough *et al.*, 'Photonic Integration for Low Size, Weight, and Power (SWaP) Remote Gas Spectroscopy', in *OSA Optical Sensors and Sensing Congress 2021 (AIS, FTS, HISE, SENSORS, ES) (2021)*, paper ETu6D.2, Optica Publishing Group, Jul. 2021, p. ETu6D.2. doi: 10.1364/ES.2021.ETu6D.2.
71. R. Shahriar, O. Hassan, and M. K. Alam, 'Adsorption of gas molecules on buckled GaAs monolayer: a first-principles study', *RSC Adv.*, vol. 12, no. 26, pp. 16732–16744, Jun. 2022, doi: 10.1039/D2RA02030K.
72. K. Xie, X. Zhang, X. Zhang, H. Jin, and J. Jian, 'A slot microring sensor with feedback spiral waveguide for trace gas CH<sub>4</sub> sensing in mid-infrared region', *Optoelectron. Lett.*, vol. 15, no. 1, pp. 1–5, Jan. 2019, doi: 10.1007/s11801-019-8107-4.
73. 'Germanium-on-Glass waveguides for Mid-IR photonics'. Accessed: Jan. 31, 2024. [Online]. Available: <https://opg.optica.org/abstract.cfm?uri=photonics-2016-Th3A.18>
74. 'Mid-infrared photonics in silicon and germanium | Nature Photonics'. Accessed: Jan. 31, 2024. [Online]. Available: <https://www.nature.com/articles/nphoton.2010.171>
75. 'Verification of Ge-on-insulator structure for a mid-infrared photonics platform'. Accessed: Jan. 31, 2024. [Online]. Available: <https://opg.optica.org/ome/fulltext.cfm?uri=ome-8-2-440&id=380890>
76. 'Sensors | Free Full-Text | Development and Measurements of a Mid-Infrared Multi-Gas Sensor System for CO, CO<sub>2</sub> and CH<sub>4</sub> Detection'. Accessed: Jan. 31, 2024. [Online]. Available: <https://www.mdpi.com/1424-8220/17/10/2221>
77. 'An integrated optic ethanol vapor sensor based on a silicon-on-insulator microring resonator coated with a porous ZnO film'. Accessed: Jan. 31, 2024. [Online]. Available: <https://opg.optica.org/oe/fulltext.cfm?uri=oe-18-11-11859&id=199658>
78. T. Jin, J. Zhou, and P. Tai Lin, 'Real-time and non-destructive hydrocarbon gas sensing using mid-infrared integrated photonic circuits', *RSC Adv.*, vol. 10, no. 13, pp. 7452–7459, 2020, doi: 10.1039/C9RA10058J.
79. N. L. Kazanskiy, S. N. Khonina, and M. A. Butt, 'Polarization-Insensitive Hybrid Plasmonic Waveguide Design for Evanescent Field Absorption Gas Sensor', *Photonic Sens.*, vol. 11, no. 3, pp. 279–290, Sep. 2021, doi: 10.1007/s13320-020-0601-6.
80. G. Mi, C. Horvath, and V. Van, 'Silicon photonic dual-gas sensor for H<sub>2</sub> and CO<sub>2</sub> detection', *Opt. Express*, vol. 25, no. 14, pp. 16250–16259, Jul. 2017, doi: 10.1364/OE.25.016250.
81. W.-Y. Wang, H.-W. Hu, J.-C. Chiou, K.-F. Yung, and C.-W. Kan, 'Poly(hexamethylene biguanide) hydrochloride (PHMB)-based materials: synthesis, modification, properties, determination, and application', *Polym. Chem.*, vol. 14, no. 48, pp. 5226–5252, Dec. 2023, doi: 10.1039/D3PY01148H.
82. 'Silicon microring refractometric sensor for atmospheric CO<sub>2</sub> gas monitoring'. Accessed: May 04, 2024. [Online]. Available: <https://opg.optica.org/oe/fulltext.cfm?uri=oe-24-2-1773&id=335762>
83. 'Polyaniline Nanofiber Gas Sensors: Examination of Response Mechanisms | Nano Letters'. Accessed: Jun. 07, 2024. [Online]. Available: <https://pubs.acs.org/doi/10.1021/nl035122e>
84. 'Sensors | Free Full-Text | Gas Sensor with Different Morphology of PANI Layer'. Accessed: Jun. 07, 2024. [Online]. Available: <https://www.mdpi.com/1424-8220/23/3/1106>
85. I. Fratoddi, I. Venditti, C. Cametti, and M. V. Russo, 'Chemiresistive polyaniline-based gas sensors: A mini review', *Sens. Actuators B Chem.*, vol. 220, pp. 534–548, Dec. 2015, doi: 10.1016/j.snb.2015.05.107.
86. A. Jain *et al.*, 'Fabrication of polypyrrole gas sensor for detection of NH<sub>3</sub> using an oxidizing agent and pyrrole combinations: Studies and characterizations', *Heliyon*, vol. 9, no. 7, p. e17611, Jul. 2023, doi: 10.1016/j.heliyon.2023.e17611.
87. W. Li, M. J. Lefferts, B. I. Armitage, K. Murugappan, and M. R. Castell, 'Polypyrrole Percolation Network Gas Sensors: Improved Reproducibility through Conductance Monitoring during Polymer Growth', *ACS Appl. Polym. Mater.*, vol. 4, no. 4, pp. 2536–2543, Apr. 2022, doi: 10.1021/acsapm.1c01819.
88. C. M. Bhatt and N. Jampana, 'Comparative studies on electrical properties of Polypyrrole based gas sensor', in *2011 IEEE Sensors Applications Symposium*, San Antonio, TX, USA: IEEE, Feb. 2011, pp. 131–135. doi: 10.1109/SAS.2011.5739793.
89. K. Nagashima, M. Kamaya, and E. Ishii, 'Electrochemical gas sensors using electrolytic films of poly(ethylene oxide)/Zn, Cu, Ni trifluoromethane sulphonates for flow injection analysis of nitrogen dioxide', *Sens. Actuators B Chem.*, vol. 9, no. 2, pp. 149–154, Aug. 1992, doi: 10.1016/0925-4005(92)80208-F.
90. K. Nagashima, K. Meguro, and T. Hobo, 'A galvanic gas sensor using poly(ethylene oxide) complex of silver trifluoromethane sulphonate electrolyte', *Fresenius J. Anal. Chem.*, vol. 336, no. 7, pp. 571–574, Jan. 1990, doi: 10.1007/BF00331419.
91. N. L. Kazanskiy, S. N. Khonina, and M. A. Butt, 'Recent Development in Metasurfaces: A Focus on Sensing Applications', *Nanomaterials*, vol. 13, no. 1, Art. no. 1, Jan. 2023, doi: 10.3390/nano13010118.
92. S. Chatterjee *et al.*, 'Hydrogen gas sensing using aluminum doped ZnO metasurfaces', *Nanoscale Adv.*, vol. 2, no. 8, pp. 3452–3459, Aug. 2020, doi: 10.1039/D0NA00289E.
93. M. A. Butt, S. N. Khonina, N. L. Kazanskiy, and R. Piramidowicz, 'Hybrid metasurface perfect absorbers for temperature and biosensing applications', *Opt. Mater.*, vol. 123, p. 111906, Jan. 2022, doi: 10.1016/j.optmat.2021.111906.

94. F. A. A. Nugroho *et al.*, 'Inverse designed plasmonic metasurface with parts per billion optical hydrogen detection', *Nat. Commun.*, vol. 13, no. 1, p. 5737, Sep. 2022, doi: 10.1038/s41467-022-33466-8.
95. 'Polymers | Free Full-Text | Towards Highly Efficient Nitrogen Dioxide Gas Sensors in Humid and Wet Environments Using Triggerable-Polymer Metasurfaces'. Accessed: Jun. 08, 2024. [Online]. Available: <https://www.mdpi.com/2073-4360/15/3/545>
96. I. Kim *et al.*, 'Holographic metasurface gas sensors for instantaneous visual alarms', *Sci. Adv.*, vol. 7, no. 15, p. eabe9943, Apr. 2021, doi: 10.1126/sciadv.abe9943.
97. 'Sensors | Free Full-Text | Metasurfaces for Sensing Applications: Gas, Bio and Chemical'. Accessed: Jun. 06, 2024. [Online]. Available: <https://www.mdpi.com/1424-8220/22/18/6896>
98. N. L. Kazanskiy, S. N. Khonina, and M. A. Butt, 'Metasurfaces: Shaping the future of photonics', *Sci. Bull.*, Apr. 2024, doi: 10.1016/j.scib.2024.04.056.
99. F. Warken, E. Vetsch, D. Meschede, M. Sokolowski, and A. Rauschenbeutel, 'Ultra-sensitive surface absorption spectroscopy using sub-wavelength diameter optical fibers', *Opt. Express*, vol. 15, no. 19, pp. 11952–11958, Sep. 2007, doi: 10.1364/OE.15.011952.
100. R. A. Potyrailo, S. E. Hobbs, and G. M. Hieftje, 'Near-Ultraviolet Evanescent-Wave Absorption Sensor Based on a Multimode Optical Fiber', *Anal. Chem.*, vol. 70, no. 8, pp. 1639–1645, Apr. 1998, doi: 10.1021/ac970942v.
101. E. Benito-Peña, M. G. Valdés, B. Glahn-Martínez, and M. C. Moreno-Bondi, 'Fluorescence based fiber optic and planar waveguide biosensors. A review', *Anal. Chim. Acta*, vol. 943, pp. 17–40, Nov. 2016, doi: 10.1016/j.aca.2016.08.049.
102. J. R. Epstein and D. R. Walt, 'Fluorescence-based fibre optic arrays: a universal platform for sensing', *Chem. Soc. Rev.*, vol. 32, no. 4, pp. 203–214, Jun. 2003, doi: 10.1039/B300617D.
103. L. Ding, P. Gong, B. Xu, and Q. Ding, 'An Optical Fiber Sensor Based on Fluorescence Lifetime for the Determination of Sulfate Ions', *Sensors*, vol. 21, no. 3, Art. no. 3, Jan. 2021, doi: 10.3390/s21030954.
104. R. B. Thompson, 'Fluorescence-Based Fiber-Optic Sensors', in *Topics in Fluorescence Spectroscopy: Principles*, J. R. Lakowicz, Ed., Boston, MA: Springer US, 2002, pp. 345–365. doi: 10.1007/0-306-47058-6\_7.
105. O. S. Wolfbeis and H. E. Posch, 'Fibre-optic fluorescing sensor for ammonia', *Anal. Chim. Acta*, vol. 185, pp. 321–327, Jan. 1986, doi: 10.1016/0003-2670(86)80060-5.
106. C. Zhang, Z. Liu, C. Cai, Z. Yang, and Z.-M. Qi, 'Surface plasmon resonance gas sensor with a nanoporous gold film', *Opt. Lett.*, vol. 47, no. 16, pp. 4155–4158, Aug. 2022, doi: 10.1364/OL.461408.
107. 'Sensors | Free Full-Text | Research Advances on Fiber-Optic SPR Sensors with Temperature Self-Compensation'. Accessed: Jun. 08, 2024. [Online]. Available: <https://www.mdpi.com/1424-8220/23/2/644>
108. 'Sensors | Free Full-Text | A Review: Application and Implementation of Optic Fibre Sensors for Gas Detection'. Accessed: Jun. 08, 2024. [Online]. Available: <https://www.mdpi.com/1424-8220/21/20/6755>
109. X. Chen, L. Gan, and X. Guo, 'Optical Fiber-Based Gas Sensing for Early Warning of Thermal Runaway in Lithium-Ion Batteries', *Adv. Sens. Res.*, vol. 2, no. 12, p. 2300055, 2023, doi: 10.1002/adsr.202300055.
110. 'Photoacoustic Spectroscopy Gas Detection Technology Research Progress - Shuidong Xiong, Xiangyu Yin, Qi Wang, Ji Xia, Ziqiang Chen, Hongwei Lei, Xin Yan, Aisong Zhu, Fengmei Qiu, Binhai Chen, Qiaoyun Wang, Lei Zhang, Keke Zhang, 2024'. Accessed: Jun. 08, 2024. [Online]. Available: <https://journals.sagepub.com/doi/10.1177/00037028231208712>
111. T. Yang, W. Chen, and P. Wang, 'A review of all-optical photoacoustic spectroscopy as a gas sensing method', *Appl. Spectrosc. Rev.*, Feb. 2021, Accessed: Jun. 08, 2024. [Online]. Available: <https://www.tandfonline.com/doi/full/10.1080/05704928.2020.1760875>
112. X. Zhang *et al.*, 'A compact portable photoacoustic spectroscopy sensor for multiple trace gas detection', *J. Appl. Phys.*, vol. 131, no. 17, p. 174501, May 2022, doi: 10.1063/5.0088257.
113. S. Qiao *et al.*, 'Ultra-highly sensitive dual gases detection based on photoacoustic spectroscopy by exploiting a long-wave, high-power, wide-tunable, single-longitudinal-mode solid-state laser', *Light Sci. Appl.*, vol. 13, no. 1, p. 100, May 2024, doi: 10.1038/s41377-024-01459-5.
114. S. Qiao *et al.*, 'A Sensitive Carbon Dioxide Sensor Based on Photoacoustic Spectroscopy with a Fixed Wavelength Quantum Cascade Laser', *Sensors*, vol. 19, no. 19, Art. no. 19, Jan. 2019, doi: 10.3390/s19194187.
115. Z. L. Wang, C. W. Tian, Q. Liu, J. Chang, Q. D. Zhang, and C. G. Zhu, 'Wavelength modulation technique-based photoacoustic spectroscopy for multipoint gas sensing', *Appl. Opt.*, vol. 57, no. 11, pp. 2909–2914, Apr. 2018, doi: 10.1364/AO.57.002909.
116. A. Elia, C. Di Franco, P. M. Lugarà, and G. Scamarcio, 'Photoacoustic Spectroscopy with Quantum Cascade Lasers for Trace Gas Detection', *Sensors*, vol. 6, no. 10, Art. no. 10, Oct. 2006, doi: 10.3390/s6101411.
117. P. Patimisco, G. Scamarcio, F. K. Tittel, and V. Spagnolo, 'Quartz-Enhanced Photoacoustic Spectroscopy: A Review', *Sensors*, vol. 14, no. 4, Art. no. 4, Apr. 2014, doi: 10.3390/s140406165.
118. M. A. Butt, 'Integrated Optics: Platforms and Fabrication Methods', *Encyclopedia*, vol. 3, no. 3, Art. no. 3, Sep. 2023, doi: 10.3390/encyclopedia3030059.
119. N. Liaros and J. T. Fourkas, 'Ten years of two-color photolithography [Invited]', *Opt. Mater. Express*, vol. 9, no. 7, p. 3006, Jul. 2019, doi: 10.1364/OME.9.003006.

120. J. E. Crowell, 'Chemical methods of thin film deposition: Chemical vapor deposition, atomic layer deposition, and related technologies', *J. Vac. Sci. Technol. A*, vol. 21, no. 5, pp. S88–S95, Sep. 2003, doi: 10.1116/1.1600451.
121. B. A. Joyce, 'Molecular beam epitaxy-fundamentals and current status', *Contemp. Phys.*, May 1990, doi: 10.1080/00107519008222015.
122. M. A. Butt *et al.*, 'Development of a low-cost silica-titania optical platform for integrated photonics applications', *Opt. Express*, vol. 30, no. 13, p. 23678, Jun. 2022, doi: 10.1364/OE.460318.
123. M. A. Butt, C. Tyszkiewicz, K. Wojtasik, P. Karasiński, A. Kaźmierczak, and R. Piramidowicz, 'Subwavelength Grating Waveguide Structures Proposed on the Low-Cost Silica–Titania Platform for Optical Filtering and Refractive Index Sensing Applications', *Int. J. Mol. Sci.*, vol. 23, no. 12, Art. no. 12, Jan. 2022, doi: 10.3390/ijms23126614.
124. Y. Chen, 'Nanofabrication by electron beam lithography and its applications: A review', *Microelectron. Eng.*, vol. 135, pp. 57–72, Mar. 2015, doi: 10.1016/j.mee.2015.02.042.
125. F. J. Hohn, 'Electron beam lithography: Its applications', *J. Vac. Sci. Technol. B Microelectron. Process. Phenom.*, vol. 7, no. 6, pp. 1405–1411, Nov. 1989, doi: 10.1116/1.584546.
126. M. Ferstl, 'Reactive ion etching: a versatile fabrication technique for micro-optical elements', in *Diffraction Optics and Micro-Optics (1998)*, paper DTuD.21, Optica Publishing Group, Jun. 1998, p. DTuD.21. doi: 10.1364/DOMO.1998.DTuD.21.
127. J. Schmitt, A. Meier, U. Wallrabe, and F. Völklein, 'Reactive ion etching (CF<sub>4</sub>/Ar) and ion beam etching of various glasses for diffractive optical element fabrication', *Int. J. Appl. Glass Sci.*, vol. 9, no. 4, pp. 499–509, 2018, doi: 10.1111/ijag.12412.
128. 'Advanced Fabrication Processes for Superconducting Very Large-Scale Integrated Circuits | IEEE Journals & Magazine | IEEE Xplore'. Accessed: Jun. 07, 2024. [Online]. Available: <https://ieeexplore.ieee.org/document/7386652>
129. S. R. Morrison, 'Selectivity in semiconductor gas sensors', *Sens. Actuators*, vol. 12, no. 4, pp. 425–440, Nov. 1987, doi: 10.1016/0250-6874(87)80061-6.
130. M. Tonezzer, S. C. Izidoro, J. P. A. Moraes, and L. T. T. Dang, 'Improved Gas Selectivity Based on Carbon Modified SnO<sub>2</sub> Nanowires', *Front. Mater.*, vol. 6, Nov. 2019, doi: 10.3389/fmats.2019.00277.
131. P. Barik and M. Pradhan, 'Selectivity in trace gas sensing: recent developments, challenges, and future perspectives', *Analyst*, vol. 147, no. 6, pp. 1024–1054, Mar. 2022, doi: 10.1039/D1AN02070F.
132. H. Wang *et al.*, 'Highly sensitive and low detection limit NO<sub>2</sub> gas sensor based on In<sub>2</sub>O<sub>3</sub> nanoparticles modified peach kernel-like GaN composites', *Sens. Actuators B Chem.*, vol. 382, p. 133452, May 2023, doi: 10.1016/j.snb.2023.133452.
133. A. Hänsel and M. J. R. Heck, 'Opportunities for photonic integrated circuits in optical gas sensors', *J. Phys. Photonics*, vol. 2, no. 1, p. 012002, Jan. 2020, doi: 10.1088/2515-7647/ab6742.
134. J. Qin *et al.*, 'Metasurface Micro/Nano-Optical Sensors: Principles and Applications', *ACS Nano*, vol. 16, no. 8, pp. 11598–11618, Aug. 2022, doi: 10.1021/acsnano.2c03310.
135. T. Allsop *et al.*, 'Photonic gas sensors exploiting directly the optical properties of hybrid carbon nanotube localized surface plasmon structures', *Light Sci. Appl.*, vol. 5, no. 2, pp. e16036–e16036, Feb. 2016, doi: 10.1038/lsa.2016.36.

**Disclaimer/Publisher's Note:** The statements, opinions and data contained in all publications are solely those of the individual author(s) and contributor(s) and not of MDPI and/or the editor(s). MDPI and/or the editor(s) disclaim responsibility for any injury to people or property resulting from any ideas, methods, instructions or products referred to in the content.